Stability of alginate scaffolds for stromal and salivary gland epithelial cell growth

By

Miriam Toro

A Master's Thesis

Submitted to College of Nanoscale Science and Engineering, State University of New York Polytechnic Institute, Albany, NY, USA

December 2022

Acknowledgments

I would like to express my deepest gratitude to my advisor, Dr. Yubing Xie. She has welcomed me into her group and provided constant support, guidance, and endless kindness during this project. I would also like to thank my committee members. Dr. Xulang Zhang, Dr. Juan Melendez, Dr. Susan Sharfstein, and Dr. Melinda Larsen for taking the time to review and assist me with my thesis, I would like to thank them for taking the time out of their busy schedules to read it and provide feedback. I would also like to thank Dr. Robert Brainard for guiding me during my first year at SUNY Polytechnic Institute (SUNY POLY) and being the first to welcome me into his lab. I would also like to thank Dr. Gregory Denbaux for guiding me with my project during my first year at SUNY POLY.

I would like to thank my labmates for taking time away from their days to train me and help me to learn and grow as a researcher.

I would also like to thank my family for their support and guidance as I progressed through my schooling over the years. I would especially like to thank my parents for pushing me through the hard times and providing me unconditional love through this experience and all others. I would like to thank my close friends for providing an ear to listen when things were not working well. I would also like to thank them for allowing me to bounce ideas off and helping me to proofread the longest paper I've ever written and give feedback.

Table of Contents

Abstract **1**

Chapter 1. INTRODUCTION **3**

1.1. Background and Significance 3

1.1.1 3D Cell Culture to Better Mimic Cellular Microenvironment. 3

1.1.2 Natural Hydrogels for 3D Cell Culture and Tissue Engineering. 4

1.1.3 Alginate Hydrogel as a Platform for Biomedical Research. 7

1.1.4 Merit of Alginate Hydrogel Microtubes for 3D Cell Culture and Tissue Engineering. 9

1.1.5 Needs of Salivary Gland Tissue Engineering Approach to Address Xerostomia and hyposalivation. 11

1.1.6 3D Culture to Recapitulate Structure and Function of Salivary Glands. 11

1.1.7 Challenges for Improving Alginate Hydrogel Stability. 13

1.2. Objectives and Expected Outcomes 14

1.3. Structure of the Thesis 17

Chapter 2. Materials and Methods. **18**

2.1. Materials. 18

2.2. Needle-in-Needle Microfluidic Device.. 18

2.3. Microfluidic Fabrication of Alginate Hydrogel Microtubes 18

2.4. Cell Culture. 19

2.5. Cell Injection and Culture in Pre-formed Alginate Hydrogel Microtubes 20

2.6. Connective Porosity. 20

2.7. Water Retention 21

2.8. Scanning Electron Microscopy. 22

2.9. Optical Imaging. 22

2.10. Live and Dead Cell Assay. 23

2.11. Culture and Release of Primary E16 Mesenchymal Cell in Alginate Hydrogel Microtubes 23

2.12. . Immunocytochemistry Analysis of the Mesenchymal Marker in Cells Released from Alginate Hydrogel Microtubes 24

Chapter 3. Results and Discussion **25**

3.1. Overview. 25

3.2. Effects of CaCl2 concentration on physical properties of alginate hydrogel microtubes 25

3.3. Effect of CaCl2 concentration on cell growth and organization in alginate hydrogel microtubes .. 34

3.4. Effects of low-temperature alginate on the stability of microtubes and cell organization in microtubes 40

3.5. Cell proliferation and Viability after Microtube Release. 45

Chapter 4. Conclusion and Future Directions **52**

4.1. Conclusions. 52

4.2. Future Directions 54

References **56**

Abstract

There is a need for understanding and recreating salivary gland stromal and epithelial cell interactions to enable simulation of the process of branching morphogenesis to create gland structure and induce polarization of salivary epithelial cells to enable gland function. Previously our lab designed a method to create biocompatible "off-the-shelf" alginate hydrogel microtubes to mimic the microenvironment of salivary gland cells. Alginate hydrogels provide a useful option for a 3D scaffold due to their biocompatibility and proven use for 3D cell culture and tissue engineering. However, alginate hydrogels, in particular, those crosslinked by Ca^{2+} are not especially stable in the presence of phosphate, which exists in cell culture media and is required for cell growth. To address the instability of alginate hydrogels due to degradation/disassociation in the presence of phosphate, $CaCl_2$ is needed to supplement the cell culture medium.

This need leads to our current focus on addressing the following two questions: i) What is the optimal minimal concentration of $CaCl_2$ to stabilize alginate hydrogel microtubes; and ii) What is the maximal $CaCl_2$ concentration that allows cells to continue to grow once released from these microtubes? In this study, $CaCl_2$ was supplemented at various concentrations between 0 mM and 50 mM (i.e., 0, 1, 2, 3.125, 6.25, 12.5, 25, and 50 mM) to determine the lowest effective concentration to stabilize alginate hydrogel microtubes while supporting cell growth and organization. The purpose of this project is to focus on the effect of $CaCl_2$ on alginate hydrogel microtube porosity and stability, as well as its effect on cell growth and regrowth after release from alginate hydrogel microtubes. We used mouse NIH 3T3 fibroblasts as model stromal cells and salivary gland epithelial SCA-9 cells as model epithelial cells to

evaluate the effects of $CaCl_2$ concentration in monoculture and also in co-culture of these cells in alginate hydrogel microtubes. By determining the optimal $CaCl_2$ concentration, we were able to maintain the structural integrity of our alginate hydrogel microtubes while allowing stromal and epithelial cells to grow, interact, and organize into cell clusters. This work lays a foundation for future organoid culture in alginate hydrogels for the salivary gland and beyond.

CHAPTER 1. INTRODUCTION

1.1. Background and Significance

1.1.1 3D Cell Culture to Better Mimic Cellular Microenvironment

The cellular microenvironment, which consists of extracellular matrix (ECM), soluble factors, and neighboring cells, plays a pivotal role in influencing cell development, organization, proliferation, differentiation and organoid formation (Watt and Hogan, 2000; Discher et al., 2005; Tortorella et al., 2022). To study cells in an environment that resembles their natural microenvironment as closely as possible, 3D cell culture techniques offer the best opportunities to study the ECM and cellular constituents of tissues, recapitulate tissue physiology and engineer functional tissues or diseased tissue models (Alsberg et al., 2002; Griffith and Swartz 2006; Hofer and Lutolf et al., 2021). Using 3D cell culture permits the study of cell behavior in vitro by mimicking the cellular microenvironment and helps to predict how the cells would behave in vivo. 3D cell culture also helps us better understand cell biology and predict clinical outcomes when compared with conventional 2D culture (Bao et al., 2018). Many of the functions of the native microenvironment, such as cell organization, cell-cell interactions, stem cell fate decision, mechanical integrity and nutrient utilization are facilitated by biomimetic ECM (Lutolf and Hubbell, 2005; Lutolf et al., 2009; Green and Elisseeff et al., 2016; Gao et al., 2022).

Cell culture has been widely used in biological studies, biomedical research, tissue engineering, regenerative medicine, and industrial use. Despite a long tradition of 2D culture, recent research has emphasized the use of 3D culture. In comparison to 2D culture, 3D culture enables cells to form structures (e.g., cellular clusters, aggregates, spheres, organoids), allowing for increased cell-to-cell contact and enhanced 3D cell-cell interaction (Fontoura et al.,2020).

3D structures are important for numerous reasons, including allowing cells to form unique aggregate structures and mimicking the cells in natural microenvironment more closely than conventional 2D culture. Cells react to chemical and biological signals as well as physical cues from their surrounding microenvironment, which imparts our ability to study cells outside of their natural environment. Therefore, 3D culture allows observations of cell-cell interactions and cell behaviors and predictions of what occurs in vivo to enable our ability to engineer tissues for regenerative therapies.

1.1.2 Natural Hydrogels for 3D Cell Culture and Tissue Engineering

Engineering a biomaterial-derived microenvironment is one of the strategies for 3D cell culture and tissue engineering. A biomaterial is a material that is designed to interact with biological systems such as cells, microbes, or tissues. Biomaterials can be used to control, adjust, or act on the various parts of a living system, for example, to promote wound healing or repair tissue damage. Biomaterials can be designed to mimic the ECM in the cellular microenvironment that surround cells in the tissue and to provide mechanical support and space for cell growth to form a new tissue (Lutolf and Hubbell, 2005). The use of biomaterials is spreading not only for therapeutic purposes but also for studying cellular processes and interactions between cells and materials in vitro since they provide control over relevant mechanical and chemical properties (Augst et al., 2006). Natural materials are gaining popularity due to their inherent biocompatibility (Lee and Mooney, 2012). The biocompatibility of biomaterials is crucial to use in a number of fields, including 3D cell culture and tissue engineering.

For 3D culture and tissue engineering, biomaterials are designed to match the bulk mechanical and structural requirements of the target tissue and to enable cell-ECM interactions at the molecular scale and promotes 3D cell growth and tissue regeneration (Place et al., 2009). Many biological interactions are difficult to study in vitro as they rely on surrounding ECM and physical interactions between the matrix and cells. Tissue engineering is a growing field with a demand for ideal biomaterials and corresponding structures to meet the needs of modeling human disorders for drug development as well as needs for human testing (Langer and Vacanti, 1993; Griffith and Naughton, 2002; Langer and Vacanti, 2016; Shafiee and Atala, 2017; Khalil et al., 2020).

In the context of biomaterials, a hydrogel is a colloidal gel in which water is the dispersion medium of the polymers. These hydrogel-forming polymers in biomedicine allow for mimicking the surrounding microenvironment of living cells and can be used in cell transplantation, tissue engineering, organ manufacturing, drug release, and pathology analysis (Jiao et al., 2022). Hydrogel can behave like the natural ECM in that they are highly hydrated 3D networks that provide a place for cells to adhere, proliferate, and differentiate (Lee and Mooney, 2001).

Hydrogels have been used in many tissue engineering applications as scaffolds to support cell attachments and provide microenvironmental cues for 3D cell culture for use in tissue regeneration, proliferation, differentiation, and function (Annabi et al., 2014). Additionally, the mechanical properties of hydrogel scaffolds can be altered by incorporating growth factors (Chu et al., 2016). Scaffolding materials are critical in guiding cell adhesion, growth, and formation of new tissues in 3D (Kuo and Ma, 2001). A hydrogel's mechanical

properties can affect both the stability of the material and the behavior of interacting cells, such as spreading, migration, and differentiation; for example, cells can sense mechanical signals through mechanosensing and transduce mechanical signals into biochemical responses (Li et al., 2018).

Natural hydrogels are the most obvious choice for scaffolds as they are naturally occurring and frequently biocompatible. Polysaccharide hydrogels are among the most explored and developed as biomaterials due to their abundance, structural diversity and functionality (Stokke, 2019). Polysaccharide hydrogels, such as alginate, chitosan, cellulose, and hyaluronic acid are derived from a wide range of natural sources, are generally biocompatible, and can be biodegraded enzymatically or through chemical hydrolysis, and can be further engineered to mimic the properties of biological tissues (Teng et al., 2021).

Hydrogels, such as alginate hydrogels that can be formed by mild gelling reactions with divalent cations (e.g., calcium ions), have been frequently used as biomimetic ECM for vascular and neural scaffolds (Raus et al., 2021) and widely used for 3D culture of homogeneous and heterogeneous mixtures of cells (Xie et al., 2022) . These alginate hydrogels are widely available, biocompatible and easily manipulated to create unique structures (Jiao et al., 2022). Hydrogels made from alginate can be prepared by various crosslinking methods, and their resemblance to glycosaminoglycan component of ECM of living cells makes them ideal for use in 3D cell culture, tissue engineering, drug and protein delivery as well as cell transplantation (Lee and Mooney, 2012).

1.1.3 Alginate Hydrogels as a Platform for Biomedical Research

Alginate hydrogels are used widely in the biomedical field and have garnered attention for their use as biomimetic ECM and in cell encapsulation for many reasons. These reasons include abundance, biocompatibility, permeability, and a rapid gelation process under mild conditions in the presence of cells (Namgung et al., 2021). Alginate is also inexpensive, non-toxic and compatible with cell survival, making it the perfect scaffolding material for cell encapsulation and 3D cell culture (Hunt et al., 2010). All of the above properties make alginate an ideal candidate for continued research with various cell types on 3D platforms that can advance the tissue engineering field and biomedical research.

Alginate generally refers to alginic acid and it salt (mostly sodium alginate). Alginic acid is insoluble, but sodium alginate is water soluble. Therefore, alginic acid is usually dissolved in sodium solution, such as 0.9% sodium chloride (physiological saline), for cell culture and biomedical application. Once encountering Ca^{2+}, sodium alginate solutions under mild conditions, forming alginate hydrogel.

Alginate is a naturally anionic polysaccharide, which is derived from brown algae's cell wall and intercellular mucilage. There are two monomeric units in the alginate polymer: (1,4)-linked β-D-mannuronate (M) residues and α-L-guluronate (G) residues (Aderibigbe and Buyana, 2018). Alginate molecules tend to have three zones, namely the "M zone" (rich in mannuronic acid), "G zone" (rich in guluronic acid), and "MG zone" (rich in both types of uronic acids) (Jiao et al., 2022). The alginate polymer may contain regions consisting exclusively of one type of monomer (M-blocks or G-blocks) or an alternating sequence of M and G residues (MG-blocks) (Ching et al.,2017). Ca^{2+} can readily bind to the "G-zone", leading to chemically crosslinking

alginates into a 3D network (Jiao et al., 2022). The gel is formed due to the affinity of alginate molecules to divalent cation ions (such as calcium ions), which cooperatively bind between G-blocks of alginate molecules, resulting in reversible ionic crosslinking described via the "egg-box" model (Sergeeva et al., 2019). This simple "egg-box" model is true for initial association and certain conditions (such as low fractional Ca^{2+} saturation and low G content) (Grant et al., 1973). Other models include co-existing lateral associate modes with increasing the fractional Ca^{2+} saturation of guluronic acid (Stokke et al., 2020) and two-component broken rod-like modes for competitive ligand exchange of chelated Ca^{2+} gelation (Yamamoto et al., 2019).

Alginate hydrogel's structures are very diverse, ranging from spherical structures, tubular structures, and scaffolding matrix structures (Xie et al., 2022). These alginate hydrogels can serve as functional substrates for cell-ECM and cell-cell interactions, providing an excellent platform for studying cell-microenvironment interactions.

The ultimate goal in tissue engineering is to allow patients suffering from loss or organ failure to obtain man-made tissue and organ replacements. In the field of tissue engineering, alginate hydrogels are promising as a scaffold for cell transplantation and the growth of the corresponding tissue or organ. Alginate hydrogels are used to deliver cells to the desired site in this approach. Their function is to provide a space for new tissue formation and to control the structure and function of engineered tissue. Their unique properties have the potential for an off-the-shelf solution for organ replacements since they have the potential to encapsulate the specific type of cells, provide appropriate ECM-mimics for the cell to form the desired tissue, and be degraded enzymatically without producing toxic waste products.

Alginate has many uses in the biomedical field for a variety of reasons which have been extensively studied, including wound healing, drug delivery, and tissue engineering applications (Lee and Mooney, 2012; Grijalvo et al., 2019; Xie et al., 2022; Zdiri et al., 2022). Since it is a naturally occurring anionic polymer and can be obtained from brown seaweed, it is naturally biocompatible and presents low toxicity when incorporated for biomedical purposes. Additional benefits of the use of alginate include relatively low cost and mild gelation by the addition of divalent cations such as Ca^{2+} (Wee and Gombotz, 1998).

The development of in vitro 3D models reconstituting in vivo physiology is essential for better understanding cell biology and predicting clinical outcomes and for designing appropriate therapeutic strategies (Namgung et al., 2021). 3D cell culture is important to accurately study cells under condition that closely resemble their natural environment. By mimicking the 3D ECM in vitro, we can better study the behavior of cells and learn how they might act in vivo (Tibbitt, Mark W., and Kristi S. Anseth.,2009). Some of the current cutting-edge techniques include utilizing alginate microtubes, microbeads or microcapsules (Zhang et al.,2009), microfibers (McNamara et al.,2017), core-shell microfibers or microtubes (Jorgensen et al. 2022), as well as other constructs (e.g., alginate electrospun nanofibers (Xue et al.,2019), porous cryoelectrospun scaffolds (Ramesh et al., 2022), cryogels (Razavi et al., 2019) and porous matrices (Lawrence and Madihally,2008).

1.1.4 Merit of Alginate Hydrogel Microtubes for 3D Cell Culture and Tissue Engineering

Within the field of alginate hydrogels, alginate hydrogel microtubes are especially useful and interesting as a vehicle to promote high density cell growth (e.g., $\geq 10^8$ cells/mL) and mass production of cell aggregates or organoids with uniform size. Alginate hydrogel in the form of a

microtubes have advantages over other structures such as spherical or bulk hydrogel structures due to easier handling, retrievable cell delivery, as well as improved 3D cell culture and tissue engineering applications. Alginate hydrogel microtubes with thin walls (≤ 200 μm) are best for these purposes and promote cell growth by facilitating the transport of oxygen and nutrients to cells from their surrounding environment. The creation of one long alginate hydrogel microfiber or microtube is ideal as it will allow for handling and retrievability compared with individual microcapsules or microbeads.

Alginate microtubes created from microfluidic blending of alginate and hyaluronic acid have been shown to consistently support long-term cell culture, producing a variety of cells in large quantity with high viability, high expansion rate and high yield. This long term culture has been demonstrated in a multitude of cell types, including human pluripotent stem cells (hPSCs), iPSC-derived cells, therapeutic T cells, and tumor-initiating cells (Li et al., 2018a; Li et al., 2018b; Lin et al., 2018a; Lin et al., 2018b; Lin et al., 2019). Alginate microtubes have shown additional benefits by their ability to facilitate cell differentiation, co-culture, or tissue reconstruction (Xie et al., 2022). The therapeutic potential of alginate hydrogel microtubes has been demonstrated by delivery of cells or implantation of hepatic fibers secreting albumin at a therapeutic level in rats (Nagata et al., 2020), islet-fibers normalizing blood glucose in diabetic mice (Onoe et al., 2013; Jun et al., 2013), MSC-fibers undergoing endothelization in mice (Liu et al., 2017) and osteogenesis in rats (Song et al., 2017), and hiPSC-derived neural ribbons exhibiting neuroprotection in rats even at the delivery dose as low as ~5,000 cells in 3-4 mm microfibers (Olmsted et al., 2020).

1.1.5 Needs of Salivary Gland Tissue Engineering Approach to Address Xerostomia and Hyposalivation

The development of functional salivary gland tissue is necessary to address both xerostomia (dry mouth), which is a common clinical symptom associated with low saliva output and hyposalivation (Jorgensen et al., 2022). There are various causes of xerostomia, including Sjögren's syndrome, autoimmune diseases, radiation therapy for head and neck cancer, diabetes, aging, and prescription drugs (Ogawa and Tsuji,2015). Patients with Xerostomia can experience various clinical problems in oral health, including dry mouth, tooth loss, dental infections, and impaired chewing and swallowing function, which cause a general reduction in quality of life (Atkinson et al., 2005). The current treatments for xerostomia include prescriptions for artificial saliva, moisturizers, and medications that induce salivation. Unfortunately, these treatments provide temporary relief of the symptoms and limited results, which cannot restore functions of salivary glands (Kagami et al., 2008). In the absence of effective treatments, there is a clinical need for a permanent solution that could be achieved using tissue engineering strategies to replace or enhance damaged or diseased salivary gland functions.

1.1.6 3D Culture to Recapitulate Structure and Function of Salivary Glands

There is great interest in examining salivary dysfunction, whether it is a symptom of a disease or a side effect of treatment (Humphrey and Williamson, 2001). The end goal of this research is to provide a platform for growing salivary glands as a treatment option for diseases impacting salivary glands such as xerostomia, which was previously described. In order to

design an appropriate platform for this growth, it is important to understand the structure and growth of the salivary gland in addition to its natural surrounding environment. From a top-level view, salivary glands consist of three major pairs, the parotid, submandibular, and sublingual. Salivary flow is primarily accomplished by the parotid and submandibular glands. While these glands are responsible for over 90% of the salivary flow, several minor salivary glands located in the oral cavity and pharynx are responsible for contributing less than 10% of this flow. The secretory unit of the salivary gland is constructed of acinar cells, myoepithelial cells, intercalated duct, striated duct and excretory duct. The acini are responsible for secreting serous (protein) and mucous (mucin) constituents of saliva. The parotid gland is a purely serous-secreting gland, whereas the submandibular is predominantly serous with 10% of the acinar cells producing mucous secretions (Bhide et al., 2009). Zooming into the cellular level, salivary gland cells are divided into two major types: epithelial and stromal cells. Salivary gland epithelial cells include acinar epithelial cells, which are secretory, secrete saliva and 85% proteins found in saliva, and ductal epithelial cells, which absorb NaCl and secrete 15% of the proteins found in saliva (Perez et al., 2010). Stromal cells interact with epithelial cells directly to support cellular organization and secretory function of salivary gland (Piraino et al., 2021).

3D cell culture and tissue engineering strategies have been used to recapitulate the structure and function of salivary gland tissues, including Matrigel (Maria et al. 2011; Hosseini et al., 2018; Koslow et al., 2019) and electrospun nanofiber scaffolds (e.g., poly (lactic co glycolic acid) (PLGA), elastin-PLGA, PLGA/poly (glycerol sebacate) (PLGA/PGS)) (Jean-Gilles et al., 2010; Sequeira et al., 2012; Cantara et al., 2012; Soscia et al., 2013; Peters et al., 2014; Foraida et al., 2017a; Foraida et al., 2017b; Sfakis et al., 2018). These cell culture systems provide valuable

platforms for studying salivary gland cell morphogenesis and function. However, Matrigel is derived from mouse tumor tissue, which limited its future applications in vivo, and most of these electrospun nanofiber scaffolds have mechanical properties that do not match those of soft tissue. To better mimic the biomechanical properties of soft tissue, alginate-elastin cryoelectrospun scaffolds and alginate hydrogel microtubes have recently been used for salivary gland cell culture (Ramesh et al., 2022; Jorgensen et al., 2022).

1.1.7 Challenges for Improving Alginate Hydrogel Stability

Alginate provides a useful option for developing 3D scaffold due to its biocompatibility and proven use for 3D cell culture and tissue engineering (Afewerki et al., 2019). However, alginate is not especially stable in the presence of phosphate that exists in cell culture media and required for cell growth. Our alginate hydrogel microtube fabrication method consists of combining 6% sodium alginate with 100 mM $CaCl_2$. This solution was used to fabricate sterile alginate hydrogel microtubes by flowing the solution through a needle-in-needle device. Alginate hydrogel microtubes were removed from 100 mM $CaCl_2$ solution prior to cell injection to these microtubes. These alginate hydrogel microtubes tended to disassociate in cell culture media during 7-14 days of cell culture (Shao et al., 2020).

To address the instability of alginate hydrogel during degradation/disassociation in the presence of phosphate, $CaCl_2$ was added to the cell culture medium. Previous work demonstrated that using 25 mM $CaCl_2$ could stabilize alginate hydrogel microtubes and scaffolds in culture for 7-14 days (Jorgensen et al., 2022; Ramesh et al., 2022). This leads to our current focus on answering the following two questions: i) What is the optimal minimal

concentration of $CaCl_2$ to stabilize alginate hydrogel microtubes? ii) What is the maximal $CaCl_2$ concentration that allows cells to continue to grow once released from the microtubes. Our trials consist of supplementing various concentrations of $CaCl_2$, from 1 mM to 50 mM, to find the lowest effective and optimal concentration to stabilize alginate hydrogels in cell culture media while allow cells to grow.

To address these questions, this project focuses on the effect of $CaCl_2$ on alginate microtube porosity and stability, as well as its effect on cell growth. We used mouse NIH 3T3 fibroblasts as model stromal cells and salivary gland epithelial SCA-9 cells as model epithelial cells to evaluate the effect of $CaCl_2$ concentration on monoculture and co-culture. Determination of the optimal $CaCl_2$ concentration will allow our alginate microtubes to maintain their structural integrity as cells grow within them.

1.2 Objectives and Expected Outcomes:

The use of a 3D scaffold can promote the directed growth and organization of stromal cells and salivary gland epithelial cells into functional organoids. The most common properties that are used in describing the characteristics and fabrications of hydrogel-based scaffolds are mechanical properties, swelling rate, pore size, porosity, nutrient exchange (e.g., glucose) ability, and biodegradability (Li et al., 2018). Alginate hydrogels with adequate properties could serve as a desirable 3D scaffold for the growth of salivary gland cells. Over the first 7 days of encapsulation, alginate-based hydrogels tend to lose their integrity due to dissociation of the divalent cation, Ca^{2+}. Although at an early stage, encapsulated cells might influence the mechanical properties of the alginate hydrogel compared to that without cells, over a longer period of culture, the hydrogel could retain sufficient mechanical integrity to exhibit gel-like

properties (Hunt et al., 2010). In the presence of supplemental $CaCl_2$, hydrogel microtubes are more stable and prevented the escape of salivary gland cells from the hydrogel microtubes. However, salivary gland cells might be sensitive to $CaCl_2$. Our aim is to determine the optimal $CaCl_2$ concentration to be added to the cell culture medium to prevent hydrogel disintegration/degradation. We studied the effects of $CaCl_2$ concentrations (1-50 mM) on alginate scaffold properties, cell viability and cell cluster formation, as well as scaffold stability in 3D cell culture. We also determined whether cells can proliferate and re-grow after being cultured in alginate hydrogel microtubes for 7 days and then released from the microtubes. Specifically, I have accomplished the following two Objectives.

Objective 1: Evaluate the effect of $CaCl_2$ on physical properties of alginate hydrogel microtubes, as well as effects on stromal and salivary gland epithelial cell growth in these microtubes.

Objective 1a: Evaluate effects of $CaCl_2$ concentration on the connective porosity and water retention of alginate hydrogel microtubes.

The concentration of $CaCl_2$ affects the porous structure, water retention and swelling characteristics of alginate hydrogel, and therefore, viability and growth of salivary gland cells. Connective porosity and water retention was measured using our established methods. The morphology of alginate hydrogel microtubes were examined under scanning electron microscopy (SEM).

Objective 1b: Evaluate the effect of $CaCl_2$ concentration on stromal and salivary gland epithelial cell growth.

Mouse NIH 3T3 fibroblasts as a stromal cell model and/or salivary gland epithelial SCA-9 cells were mono- or co-cultured in alginate hydrogel microtubes for seven days, which were supplemented with $CaCl_2$ at different concentrations (0, 1, 2, 3.125, 6.25, 12.5, 25, and 50 mM)

in a cell culture medium consisting of DMEM/F12 with 10% fetal bovine serum and 1% penicillin-streptomycin (pen/strep, 10,000 U/mL). We measured cell viability using the Live/Dead reagent and observed cell growth and organoid-like cell cluster formation under an inverted optical microscope. The effect of $CaCl_2$ concentration on cell viability and organization was discussed.

Objective 2: Determine whether salivary gland stromal cells can regrow once they have been released from the alginate hydrogel microtubes after 7 days of culture.

In order to demonstrate whether cells released from the microtubes can grow, primary embryonic day 16 (E16) mesenchymal cells were injected into alginate hydrogel microtubes and cultured for seven days. These cells were then released and plated in a 24-well plate to grow for an additional seven days. While previous work tested for mesenchymal markers suggesting that these cells retain their phenotype and ability to grow in alginate hydrogel microtubes, this work further tested the ability to regrow primary E16 mesenchymal cells for an additional 7 days while retaining mesenchymal marker vimentin after release from the microtubes. This study validates the ability of alginate hydrogel microtubes to retain stromal cell phenotype and (re)growth potential.

Expected outcomes and impacts

By successful completion of Objective 1, we expect to determine the optimal $CaCl_2$ concentration that stabilizes alginate microtubes, while having the minimum effect on the growth of stromal and epithelial cells, which will provide guidelines for cell phenotype depending on the cell line grown in the alginate microtubes. By successful completion of Objective 2, we expect to demonstrate that once released from alginate microtubes, cells

continue to proliferate and express characteristics markers, validating the usefulness of alginate hydrogel microtubes for cell maintenance, growth and organoid-like structure formation.

1.3 Structure of the Thesis

Starting with the abstract, I have laid out the significance and objectives of this research in Chapter 1 Introduction. Next, Chapter 2 describes the Materials and Methods. Chapter 3 discusses my findings related to the evaluation of the effects of $CaCl_2$ concentration on the properties of alginate hydrogel microtubes as well as the cells encapsulated within after a one-week encapsulated incubation period. For this section, I focus on the changes to the porous structure and swelling characteristics of the alginate microtubes. Regarding the effects on the cells, I focus on changes to both the viability and cellular organization of stromal cells and salivary gland cells. Additionally, I dig in deeper to the viability of the salivary gland cells as we track the cells for a longer duration to study their ability to regrow once released from their surrounding alginate hydrogel microtubes. For this part of the study, I track the potential of the cells to grow for an additional week once released. Finally, the thesis concludes with a summary section which is comprised of a summary of findings in addition to conclusions being drawn and potential future research goals and opportunities being discussed in Chapter 4, Conclusions and Future Directions.

Chapter 2 Materials and Methods

2.1. Materials

Sodium alginate and calcium chloride dihydrate ($CaCl_2 \cdot 2H_2O$) were purchased from Sigma-Aldrich (St. Louis, MO). 3 mL disposable syringes were purchased from Becton Dickinson (Franklin Lakes, NJ). 17-gauge and 22-gauge blunt-tip needles were purchased from Hamilton Company (Reno, NV). Multiple gauged premium Kanthal wires were purchased from Amazon or Walmart.

2.2. Needle-in-Needle Microfluidic Device

A needle-in-needle microfluidic device (Device 17-22) was fabricated by precisely placing a needle (22-gauge) within another needle (17-gauge) as described previously (Jorgensen et al., 2021). Briefly, the inner needle was wrapped in properly sized Kanthal wires to allow the inner needle to be centered within the outer needle. This coiled feature allows for additional mixing of the sodium alginate solution, if needed, before introduction into the $CaCl_2$ solution.

2.3. Microfluidic Fabrication of Alginate Hydrogel Microtubes.

A 100 mM $CaCl_2$ solution (core fluid), 6% sodium alginate solution (sheath fluid), and a separate 100 mM $CaCl_2$ solution (collecting fluid) were prepared in 0.9% NaCl solution, followed by autoclave sterilization. Syringes were loaded with the sheath fluid (6% sodium alginate) and core fluid (100 mM $CaCl_2$) and loaded into two NE 1000 syringe pumps (New Era Pump Systems Inc., Farmingdale, NY) which were set to optimal flow rates for microtube formation. The

syringes were connected to the needled-in-needle microfluidic device and the extrusion process was directed to extrude into a collecting pool of 100 mM $CaCl_2$ solution contained within a 50 mL conical centrifuge tube. When the sodium alginate solution converges with the $CaCl_2$ solution, immediate alginate crosslinking occurs, creating an alginate hydrogel microtube. Upon introduction into the conical tube filled with the collecting fluid (100 mM $CaCl_2$ solution), the "liquid rope-coil effect" occurs (Kuo and Ma, 2001). This effect allowed for an organized stack of alginate hydrogel microtubes for ease of storage and handling in future experiments. These pre-formed alginate microtubes were then stored at 4 °C in 50 mL conical tubes filled with 100 mM $CaCl_2$ until needed for cell culture experiments. The amount of time these microtubes were stored in the 4 °C fridge was varied from 1 to 24 hours prior to cell culture.

2.4. Connective Porosity

In order to measure the connective porosity, microtubes were extruded into the 50 ml centrifuge tube. The microtubes were lifted out of the centrifuge tube, placed into a large petri dish, and cut into 24 equal pieces of 100 mm in length. Twenty-four 35-mm cell culture dishes were individually weighed and numbered with the weight of each being recorded as W0. Each microtube was placed in a 35-mm dish without any water drops on the microtube. The weight of the 35-mm dish with the microtubes inside was recorded on day 7 (W1). The weight of the microtube was calculated as (W1-W0). Measurements in triplicate were performed by adding DMEM/F12 medium supplemented with different $CaCl_2$ concentrations (0, 1, 2, 3.125, 6.25, 12.5, 25, and 50 mM) to three dishes for each concentration. These hydrogel microtubes were

incubated for 1 hour or 7 days in an incubator with 5% CO_2. After removing all the water within the interconnected pores with a Kim wipe, the 35-mm dish with the microtube was weighed again and recorded as W2. The weight of the microtube after liquid being wicked away from connective pores was calculated by (W2-W0). Therefore, the weight of liquid wicked away from connective pores = (W1-W0) - (W2-W0) = W1-W2. Assuming the density of cell culture medium is close to water density that is 1 g/cm3 (i.e., 1 g/mL) (Poon, 2022), the volume of connective pores = (W1-W2)/(1 g/mL). The volume of these microtubes was calculated by measuring the outer diameter in µm, inner diameter equal to the outer diameter minus 2 times the wall thickness of the microtube µm, and length of 100 mm. The connective porosity (%) was calculated by dividing the volume of the connective pores by the volume of the microtube.

2.5. Water Retention

To calculate water retention, the previous measurements of the 35-mm dish (W0) and the microtube dish (W2) which were already measured from the connective porosity section were used again. Next, different $CaCl_2$ concentrations of DMEM/F12 medium were added and the microtubes filled with medium were weighed over time. After a few hours when hydrogels were saturated with the medium, all of the medium was removed from the 35-mm petri dish and the weight of the dish with the microtube was recorded as the swelling weight (Wswe). The microtubes were air-dried overnight. The dish with the dry microtube was weighed and recorded as the dry weight (Wdry). Next, we calculated the mass of the swollen hydrogel, M_S = Wswe-W0, and mass of the dried hydrogel, M_D = Wdry-W0.

Based on the following equation, the water retention, Qm was calculated:

$$Qm = \frac{M_S - M_D}{M_D} \times 100\%$$

2.6. Scanning Electron Microscopy

Scanning electron microscopy (SEM) imaging was performed using Zeiss Leo 1550 field emission SEM (Zeiss Leo Electron Microscopy Ltd, Cambridge, UK). This technique was used to image the alginate hydrogel microtubes to study their morphology with high resolution. Samples were air dried overnight and mounted on a 1.25 cm2 stub. Samples were then coated with iridium to minimize sample charging. Images were taken using an in-lens detector, 1-5kV acceleration voltage and a working distance of 2-6 mm. The microscope annotation software was used to apply scale bars and most SEM images were captured using 100x - 200x magnification.

2.7. Cell Culture

Mouse NIH 3T3 fibroblasts were used as a model of stromal cells and salivary gland epithelial SCA-9 cells were used as a model of epithelial cells. Both NIH 3T3 fibroblasts and SCA-9 cells were kindly provided by Professor Melinda Larsen from University at Albany, SUNY, and grown in culture media composed of high glucose Dulbecco's Modified Eagle's Medium (DMEM) (Sigma-Aldrich), supplemented with 10% fetal bovine serum (FBS) (Sigma-Aldrich) and 1% penicillin-streptomycin (pen/strep, 10,000 units penicillin and 10 mg streptomycin per mL) (Sigma-Aldrich). Cells were cultured in a 37 °C, 5% CO_2 humidified incubator and subcultured by trypsinization and replating every 2-3 days for NIH 3T3 fibroblasts or every 4-5 days for SCA-9 cells. The medium was typically replaced every other day.

2.8. Cell Injection and Culture in Pre-formed Alginate Hydrogel Microtubes

For monoculture in alginate hydrogel microtubes, NIH 3T3 fibroblasts or salivary gland epithelial SCA-9 cells (at a density of 5×10^6 cells/mL) were transferred into a syringe with a 22-gauge blunt needle attached. For co-culture in hydrogel microtubes, SCA-9 cells and NIH 3T3 fibroblasts were mixed at a ratio of 1:5 to obtain a final cell density of 3×10^6 cells/mL in a 1 mL cell mixture. To achieve the epithelial to mesenchymal ratio of 1:5 for co-culture, SCA-9 cells were mixed with NIH 3T3 cells by combining 0.1 mL SCA-9 (5×10^6 cells/mL) and 0.5 mL NIH 3T3 cells (5×10^6 cells/mL) with an additional 0.4 mL culture medium. For each cell solution, the syringe was positioned so that the needle could be inserted into the open end of the 1 cm long alginate hydrogel microtube, and then cells were injected into the microtube. After cell injection, 1 cm hydrogel microtubes were placed in each well of three separate 24-well plates. Each plate containing alginate microtubes was cultured in DMEM/F12 medium, supplemented with 10% FBS, 1% pen/strep under a CO_2 humidified atmosphere at 37 °C. To study the effects of $CaCl_2$, the media was supplemented with $CaCl_2$ to create eight concentrations (0, 1, 2, 3.125, 6.25, 12.5, 25, and 50 mM). The eight concentrations were used in each of the three 24 well plates. The medium was changed every other day.

2.9. Optical Imaging

A Nikon TS100 inverted microscope (Micro Video Instruments, Foxborough, MA) was used to monitor cell growth in hydrogel microtubes daily. was used to image alginate hydrogel microtubes. Images of cell growth in alginate hydrogel microtubes on days 1, 3, and 7 were

taken with a 4x objective lens using AMG EVOS FL microscope (Thermo Fisher Scientific, Waltham, MA).

2.10. Live and Dead Cell Assay

After aspirating the medium from each well, cells in the 24-well plate were stained with Live/Dead cell stain solution, composed of calcein-AM and ethidium homodimer-1 (EthD). The live/dead cell stain solution was prepared by adding 10 µL of 1 mg/mL calcein AM stock solution and 12.5 µL of 1 mg/mL EthD solution to 5 mL of DMEM/F12. 500 µl of Live/Dead cell stain solution was added to each well containing alginate hydrogel microtubes with cell-containing clusters. The well plates were then incubated at 37°C for 20 minutes. Images were taken using AMG EVOS FL microscope.

2.11. Culture and Release of Primary E16 Mesenchymal Cell in Alginate Hydrogel Microtubes

Primary E16 mesenchymal cells were isolated from mouse salivary submandibular glands as described previously (Jorgensen et al., 2022). Primary E16 cells were cultured in Gibco DMEM/F-12 medium supplemented with 10% FBS, 1% pen/strep (Sigma Aldrich). These cells were injected into alginate hydrogel microtubes as described in section 2.5. Primary E16 mesenchymal cells were cultured in microtubes for 7 days and on the 7^{th} day of culturing, cell clusters were released from the microtube by dissolving the alginate hydrogel with 1.6% sodium citrate solution (Sigma-Aldrich). The released cell clusters were then collected in a 24-well plate with a coverslip inside each well and incubated for an additional 7 days with optical images being taken on the subsequent day 1, day 4 and day 7 using AMG EVOS FL microscope.

2.12. Immunocytochemistry Analysis of the Mesenchymal Marker Vimentin in Cells Released from Alginate Hydrogel Microtubes

On day 7 after release from the alginate microtubes, the primary E16 mesenchymal cells on glass coverslips were fixed with 4% paraformaldehyde (PFA, Sigma-Aldrich) in PBS for 30 minutes at room temperature. Samples were rinsed with 1x PBS-Tween (0.1% Tween 20 in 1x PBS, Fisher Thermo Scientific, Fair Lawn, NJ) three times and permeabilized using 0.1% Triton X-100 (Sigma-Aldrich) in PBS for 15 min at room temperature. After rinsing again with PBS-Tween three times, samples were placed in blocking solution in a 4 °C fridge on a rocker for 1 hour. The blocking solution was composed of 5% bovine serum albumin (BSA, Sigma Aldrich) in PBS. After removal of excess blocking solution, the primary antibody Alexa Fluor® 488-conjugated anti-vimentin (1:100, Cell Signaling Technology, Danvers, MA) prepared in blocking solution containing DAPI (4',6-diamidino-2-phenylindole, Sigma-Aldrich) was added to samples and incubated overnight at 4 °C on a rocker. The following day, samples were rinsed three times using 1x PBS-Tween. Samples were then observed and imaged on a Leica Confocal Microscope TCS SP-5 controlled by LAS-AF software using 10x (dry) and 63x (oil immersion) objectives (Leica Microsystems, Mannheim, Germany) excited by the argon 488 laser for vimentin and excited by the 405 Diode laser at for DAPI detection.

Chapter 3 Results and Discussion

3.1. Overview

Alginate hydrogel microtubes have great potential to advance 3D cell culture, cell delivery, and tissue engineering strategies (Xu et al., 2021). However, one of the big challenges in using alginate hydrogel microtubes is maintaining their integrity and stability due to the dissociation of Ca^{2+} from alginate hydrogels in cell culture medium. Supplementing with 25 mM $CaCl_2$ in cell culture media was previously observed to stabilize the alginate hydrogel microtubes (Jorgensen et al., 2021). To further optimize and identify the minimal $CaCl_2$ concentration to maintain alginate hydrogel integrity and support cell culture, we set out to study the effect of varying concentrations of supplemental $CaCl_2$ (1-50 mM) in medium on alginate hydrogel microtube properties such as connective porosity and water retention as well as cell growth in these microtubes created from alginate solution that was equilibrated to room temperature or alginate solution that was chilled to 4 °C prior to the microtube creation process.

3.2. Effects of $CaCl_2$ concentration on physical properties of alginate hydrogel microtubes

First, we created hydrogel microtubes from a room-temperature alginate solution. We prepared alginate hydrogel microtubes in a sterile manner by infusing 6% sodium alginate and 100 mM $CaCl_2$ through a needle-in-needle device (Device 17-22) as described previously (Jorgensen et al., 2021) into a sterile 50 mL centrifuge tube containing 100 mM $CaCl_2$. These alginate hydrogel microtubes were transferred into 35 mm Petri dishes with cell culture medium (e.g., DMEM/F12 medium containing 1.05 mM $CaCl_2$), supplemented with 0 mM, 1

mM, 2 mM, 3.125 mM, 6.25 mM, 12.5 mM, 25 mM, and 50 mM $CaCl_2$, respectively. The effect of $CaCl_2$ concentration on properties of alginate hydrogel microtubes was studied, including connective porosity, water retention, and microtube morphology.

The first characteristic that we set out to study was the connective porosity of alginate hydrogel microtubes at different $CaCl_2$ concentrations. One impact of the $CaCl_2$ on the porosity of the hydrogel could be on the mechanical properties, with stiffness decreasing as porosity increases, and fluid flux caused by deformation affecting the mechanical properties of the microtubes (Annabi et al., 2010). Another impact of the $CaCl_2$ could be that the change in porosity could affect oxygen and nutrient transport into the hydrogel and the diffusion of cell products such as proteins outside the hydrogel (Andersen et al., 2015). The results obtained for connective porosity as a function of increasing $CaCl_2$ concentration were evaluated after incubation for 1 hour (Figure 3.1 A) and on day 7 (Figure 3.1 B). We found that the connective porosity of alginate hydrogel microtubes decreased from ~75% to ~25% with an increase in $CaCl_2$ concentration from 0 mM to 50 mM supplemented in media for 1 hour. After 7 days of incubation the connective porosity of alginate hydrogel microtubes decreased from ~65% to ~20% when $CaCl_2$ concentration in media increased from 0 mM to 50 mM. When $CaCl_2$ concentration was at 6.25 mM, the connective porosity of alginate hydrogel microtubes was around 40% for 1-hour incubation and decreased to 25% for 7-day incubation. When $CaCl_2$ concentration was higher than 6.25 mM, there was no significant change in the connective porosity, which is ~20% after 7 days of incubation. The relationship between the pore size and crosslinking divalent cations, such as Ca^{2+}, Sr^{2+} and Ba^{2+} ions has previously been investigated. It was demonstrated that Ca^{2+} could bind to G- and MG-blocks, Ba^{2+} to G- and M-blocks, and

Sr^{2+} to G-blocks solely; Ba^{2+} produced hydrogels with reduced pore size due to its higher affinity for G-blocks (Kierstan et al., 1982) while Sr^{2+} gave rise to alginate hydrogels with characteristics lying between Ca^{2+} and Ba^{2+} (Mørch et al., 2006). Our results with Ca^{2+} reinforce the decreased porosity as the concentration of a crosslinking divalent cation is increased.

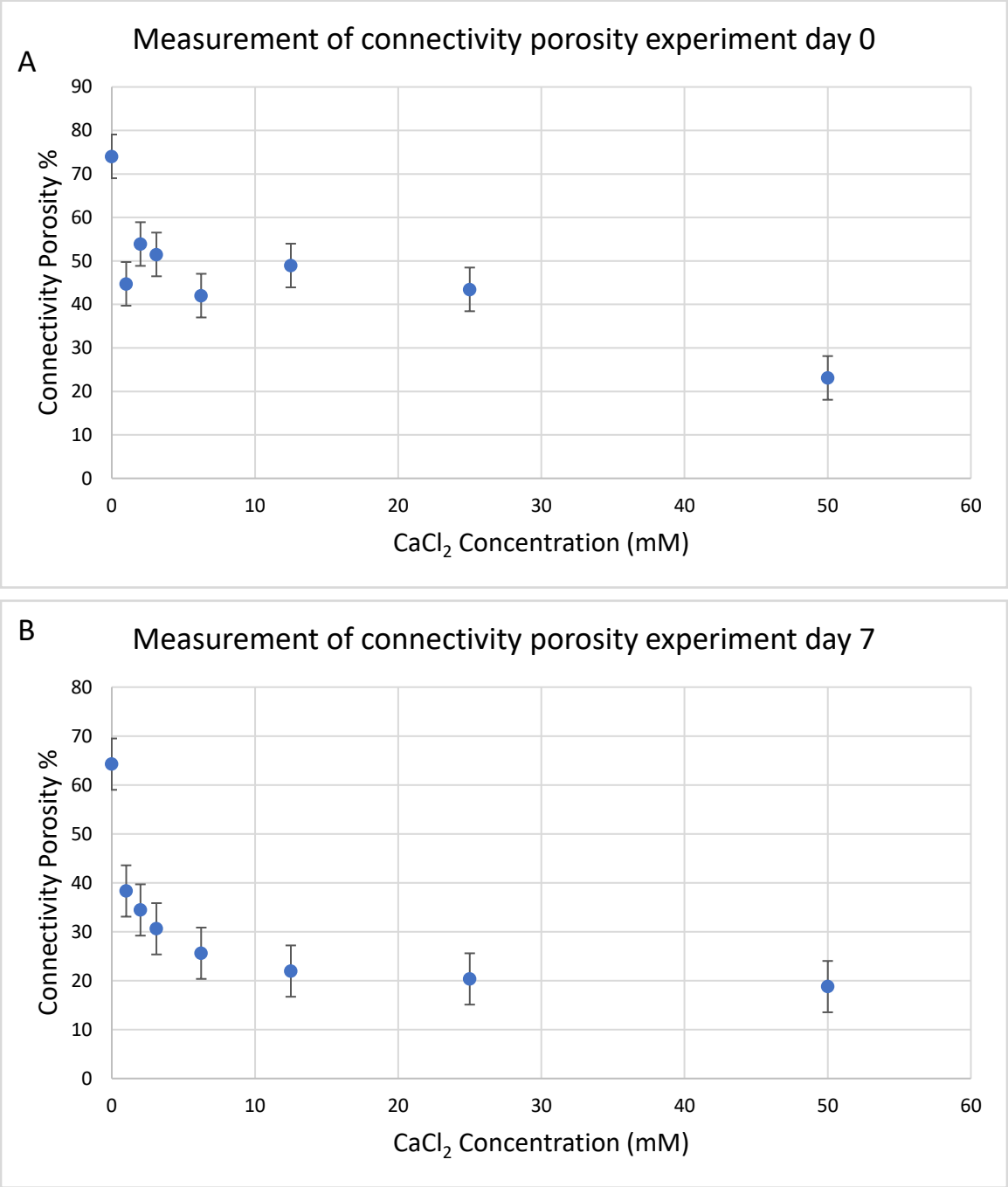

Figure 3.1. Effect of $CaCl_2$ concentration on connective porosity of alginate hydrogel microtubes. (A) After incubation for 1 hour. (B) After incubation for 7 days.

To further evaluate the effect supplementary of $CaCl_2$ concentration in the medium, we next studied the water retention of alginate microtubes as a function of the concentration of supplemented $CaCl_2$. We then measured 100 mm alginate hydrogel microtubes samples in pre-weighed 35 mm Petri dishes. Next, these hydrogels were immersed in either medium alone or medium supplemented with $CaCl_2$ at eight different concentrations (0, 1, 2, 3.125, 6.25, 12.5, 25, and 50 mM) at 37°C for 1 hour (Day 0) or seven days (Day 7). Following the 1-hour or seven-day incubation, these hydrogels were removed from the medium and their mass was measured. These hydrogels were air-dried for 24 hours to obtain the mass of the dried hydrogel microtubes. Based on the following equation, the water retention was calculated:

$$Qm = \frac{M_S - M_D}{M_D} \times 100\%$$

In this equation, Qm represents the water retention, Ms represents the mass of the swollen hydrogel after 1 hour or 7 days of incubating in DMEM at 37°C, and M_D represents the mass of the dried hydrogel.

We evaluated the water retention as a function of $CaCl_2$ concentration supplemented to media after 1 hour or 7 days (Figure 3.2). After 1 hour of incubation, the water retention was in the range of 2.5% to 7% (Figure 3.2 A). When the $CaCl_2$ concentration was lower than 6.25 mM, the water retention stayed around 3-4%. When $CaCl_2$ concentration was higher than 6.25 mM, the water retention rate increased with the increasing $CaCl_2$ concentration. After 7 days of incubation, the water retention ratio of alginate hydrogel microtubes increased from 2.5% to 8% with the increase of $CaCl_2$ concentration as well (Figure 3.2 B). We found that low $CaCl_2$ concentrations, between 0 mM and 6.25 mM, resulted in a low amount of water retention

possibly due to a low crosslinking density in the alginate hydrogel. This lower crosslinking density results in easy loss of water inside the microtubes and allows for disassociation of the alginate hydrogel to readily occur. As $CaCl_2$ concentrations increased in the medium, between 12.5 mM and 50 mM, a greater amount of the water was retained due to a higher crosslinking density. Overall, when $CaCl_2$ concentration was increased, the water retention generally increased. In particular, these data suggest the ability of 12.5-50 mM $CaCl_2$ to stabilize alginate hydrogel microtubes.

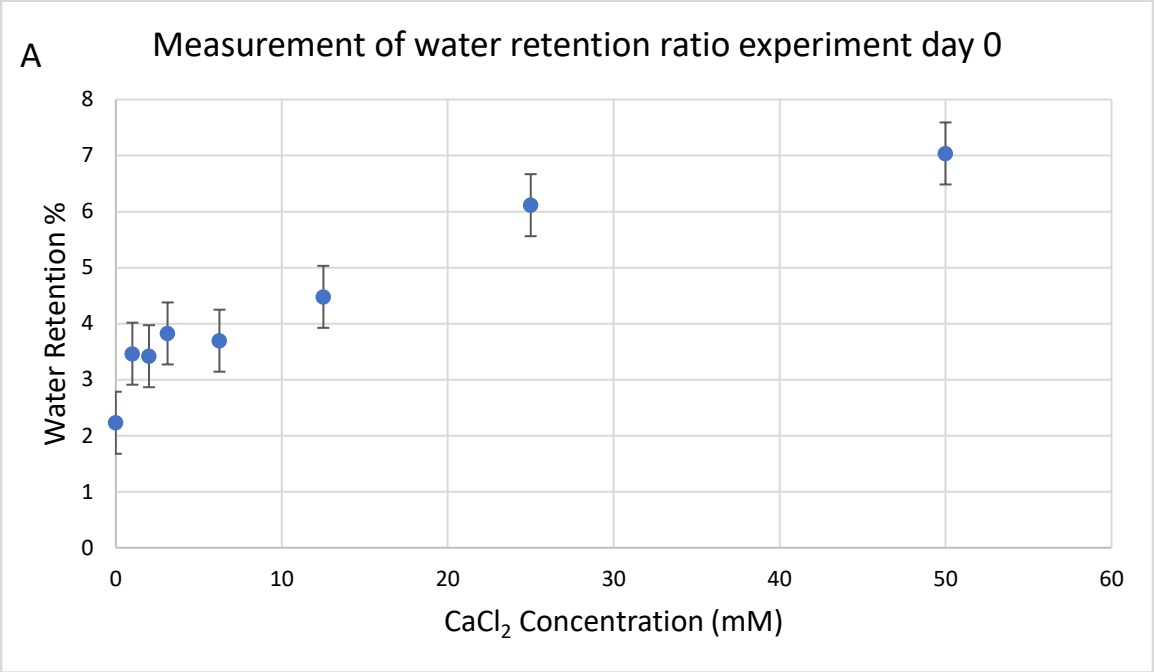

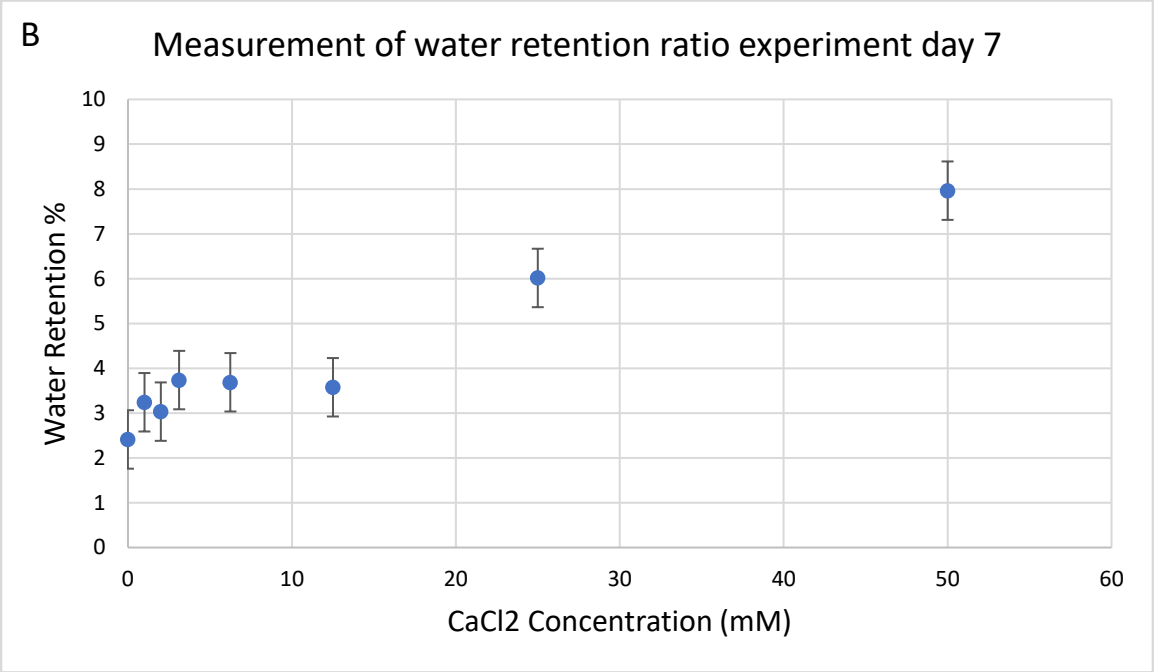

Figure 3.2. Effect of $CaCl_2$ concentration on water retention by alginate hydrogel microtubes. (A) After incubation for 1 hour. (B) After incubation for 7 days.

To confirm the influence of $CaCl_2$ on pore structure at different concentrations, we further used SEM to observe the surface morphology of alginate hydrogel microstrands after incubation with 0-50 mM $CaCl_2$ for 1 hour (Figure 3.3 A) and 7 days (Figure 3.3B). Without any $CaCl_2$ supplementation into the medium, the alginate hydrogel microtube showed a smooth surface morphology (Figure 3.3A, 0 mM). After incubation in medium supplemented with $CaCl_2$ (1-50 mM) for 1 hour, obvious changes in surface morphology of the alginate hydrogels were observed (Figure 3.3A), suggesting the interaction of supplemented $CaCl_2$ with the alginate hydrogel. In particular, $CaCl_2$ at concentrations of 12.5-50 mM exhibited less pore structures compared to 1 mM $CaCl_2$, which may partially explain lowered connective porosity with increased $CaCl_2$ concentration as seen in Figure 3.2A. After 7 days of incubation, alginate hydrogel microtubes were not stable enough for SEM sample preparation when $CaCl_2$ was 3.125 mM and below. When incubated with $CaCl_2$ at the concentration of 6.25 mM and above, alginate hydrogel microtubes on day 7 maintained their integrity and showed more crosslinked, denser structures at higher $CaCl_2$ concentration (Figure 3.3B) compared to their counterparts at 1 hour (Figure 3.3A).

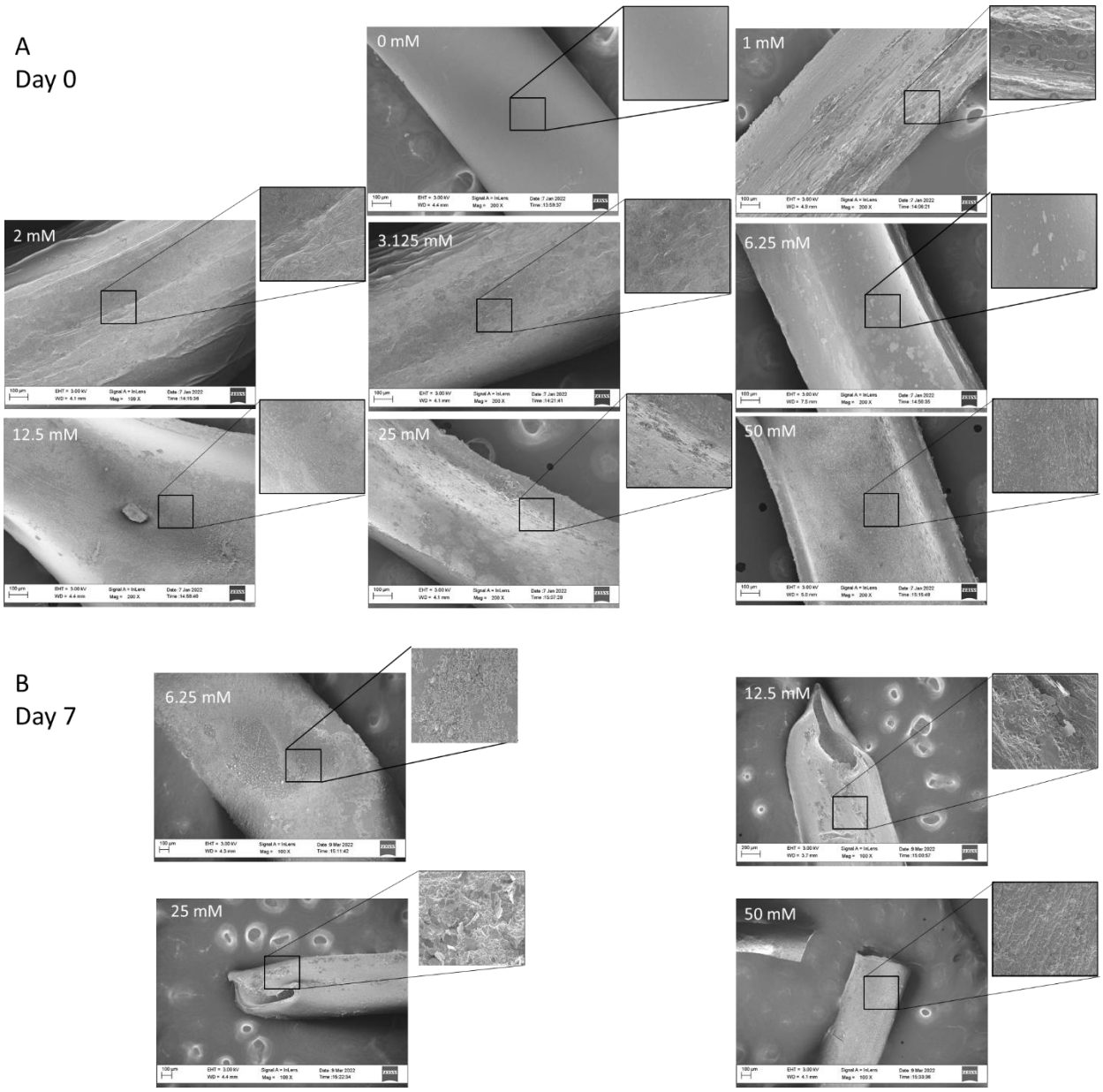

Figure 3.3. SEM images of alginate hydrogel microtubes incubated with 0, 1, 2, 3,125, 6.25, 12.5, 25, and 50 mM $CaCl_2$. (A) After incubation for 1 hour. Scale bar = 100 µm. (B) After incubation for 7 days. Scale bar = 100 µm.

3.3. Effect of $CaCl_2$ concentration on cell growth and organization in alginate hydrogel microtubes

In our next set of experiments, we examined the effects of $CaCl_2$ concentration on the growth of stromal cells and salivary gland epithelial cells. Alginate-based hydrogels tended to lose their integrity after 7 days of incubation due to the loss of Ca^{2+} from the hydrogel and degradation of the hydrogel in media. To reduce the degradation that occurs as alginate-based hydrogels lose Ca^{2+}, we tested different concentrations of $CaCl_2$ supplementation in the cell culture media used to incubate encapsulated NIH 3T3 fibroblasts and SCA-9 salivary gland epithelial cells.

The alginate solution was allowed to reach room temperature after being removed from the refrigerator at 4 °C. By using the previously described method, alginate hydrogel microtubes were formed and cells were injected into them. These hydrogel microtubes were then placed in DMEM (containing 1.8 mM $CaCl_2$) supplemented with different concentrations of $CaCl_2$ (0-50 mM) and monitored over the course of 7 days. Microtubes observed under a microscope were imaged for structural stability and consistency on days 1, 3 and 7 (Figure 3.4),

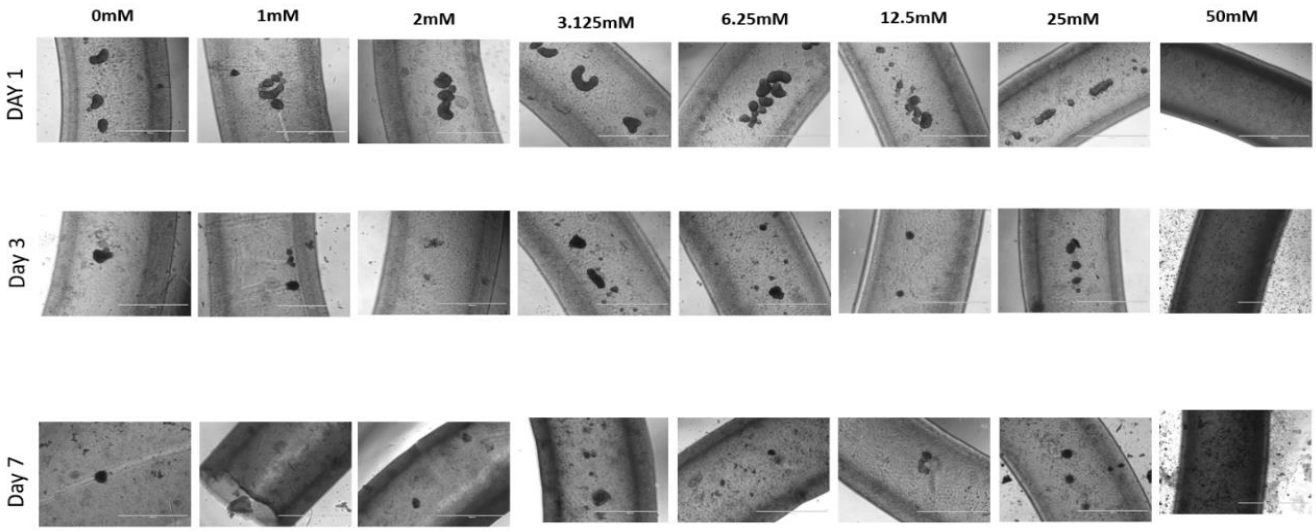

Figure 3.4. An optical image on days 1, 3, and 7 illustrating the effect of CaCl2 concentration on NIH 3T3 cell morphology grown in alginate hydrogel microtubes. Scale bar = 1000 μm.

demonstrating the feasibility of monitoring the stability of the microtube and organization behavior of encapsulated NIH 3T3 fibroblasts. Images of NIH 3T3 fibroblasts cultured in alginate hydrogel microtubes supplemented with $CaCl_2$ at 0-25 mM taken on day 1 showed formation of cell clusters within the microtube. Each subsequent image shows fewer cells within the microtube, suggesting that the cells might migrate out of the ends of the microtubes over time. The higher the $CaCl_2$ concentration, the more stable alginate hydrogel microtubes, however, 50 mM $CaCl_2$ did not support cell growth or cell cluster formation.

The previously described experiment was repeated with the addition of Live/Dead staining on day 7 to validate cell viability (Figure 3.5). After 7 days of cultivation, most cells showed the ability to convert calcein AM to positive calcein staining with strong green fluorescence, indicating that they were viable in all hydrogels. EthD-1 staining revealed only a few dead cells in red fluorescence, indicating that these microtubes were keeping most cells alive and viable despite the presence of additional $CaCl_2$ at higher concentrations.

Subsequently, three different cell types were used to examine cell organization/cluster formation in alginate hydrogel microtubes when cultured in media supplemented with 0-50 mM $CaCl_2$, including the model stromal cells, NIH 3T3 fibroblasts (Figure 3.5), salivary gland epithelial cells, SCA-9 cells (Figure 3.6), and a co-culture of SCA-9 salivary gland epithelial cells and NIH 3T3 fibroblasts at an epithelial to stromal cell ratio of 1:5 (Figure 3.7). Figure 3.5A shows cell clusters within the microtube on day 7 for 2-25 mM concentrations in the optical images. Repeated iterations of this experiment have demonstrated cell self-organization forms

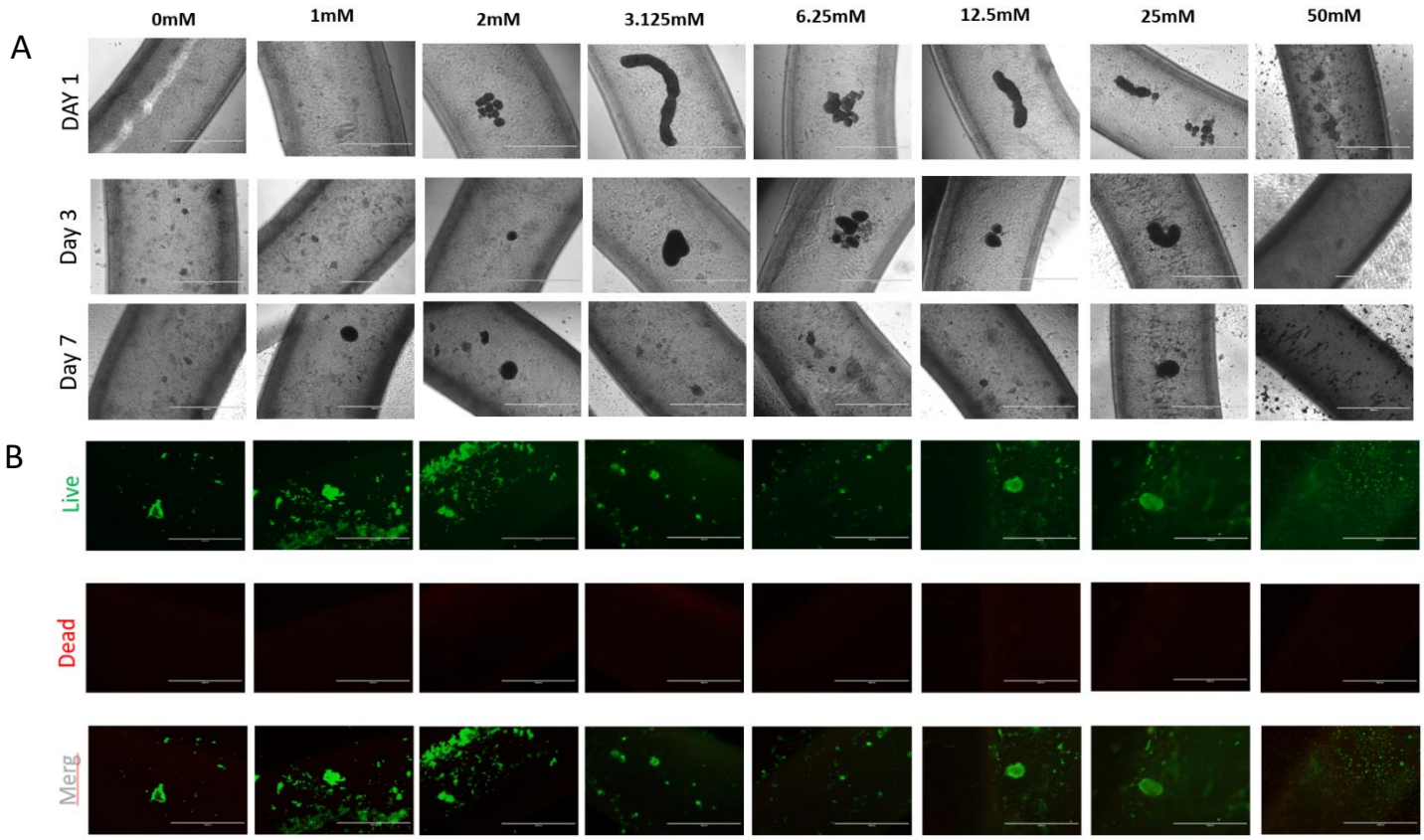

Figure 3.5. Effects of $CaCl_2$ concentration on cell morphology and viability of NIH 3T3 cells grown in alginate hydrogel microtubes made of alginate at room temperature. (A) Optical images on days 1, 3 and 7. Scale bar = 1000 μm. (B) Fluorescence of Live/Dead stained cells on day 7. Green: live cells. Red: dead cells. Scale bar = 1000 μm.

as early as the day of injection, but with an undesirable fusion of clusters occurring by day 1. This undesirable fusion was associated with the likelihood of cell migration outside from the end of the microtube by day 7. Live/Dead staining showed that NIH 3T3 fibroblasts formed viable cell clusters on day 7 when supplemented with 12.5 mM $CaCl_2$ as well as 25 mM $CaCl_2$ (Figure 3.5B). With $CaCl_2$ concentrations lower than 6.25 mM, separated cell clusters appeared to occur less reliably. This result suggests that higher $CaCl_2$ concentration (e.g., 12.5 mM, 25 mM) could provide the best balance of providing Ca^{2+} ions to promote alginate stability, while also providing a suitable environment for cell growth and organization. However, for this

experiment, NIH 3T3 fibroblasts did not form uniform cell clusters in alginate hydrogel microtubes.

In the next iteration of this experiment, when salivary gland epithelial SCA-9 cells were cultured in alginate hydrogel microtubes as shown in figure 3.6, they did not form clusters on day 1 except when supplemented with 3.125 mM and 12.5 mM $CaCl_2$. Cells of this type were

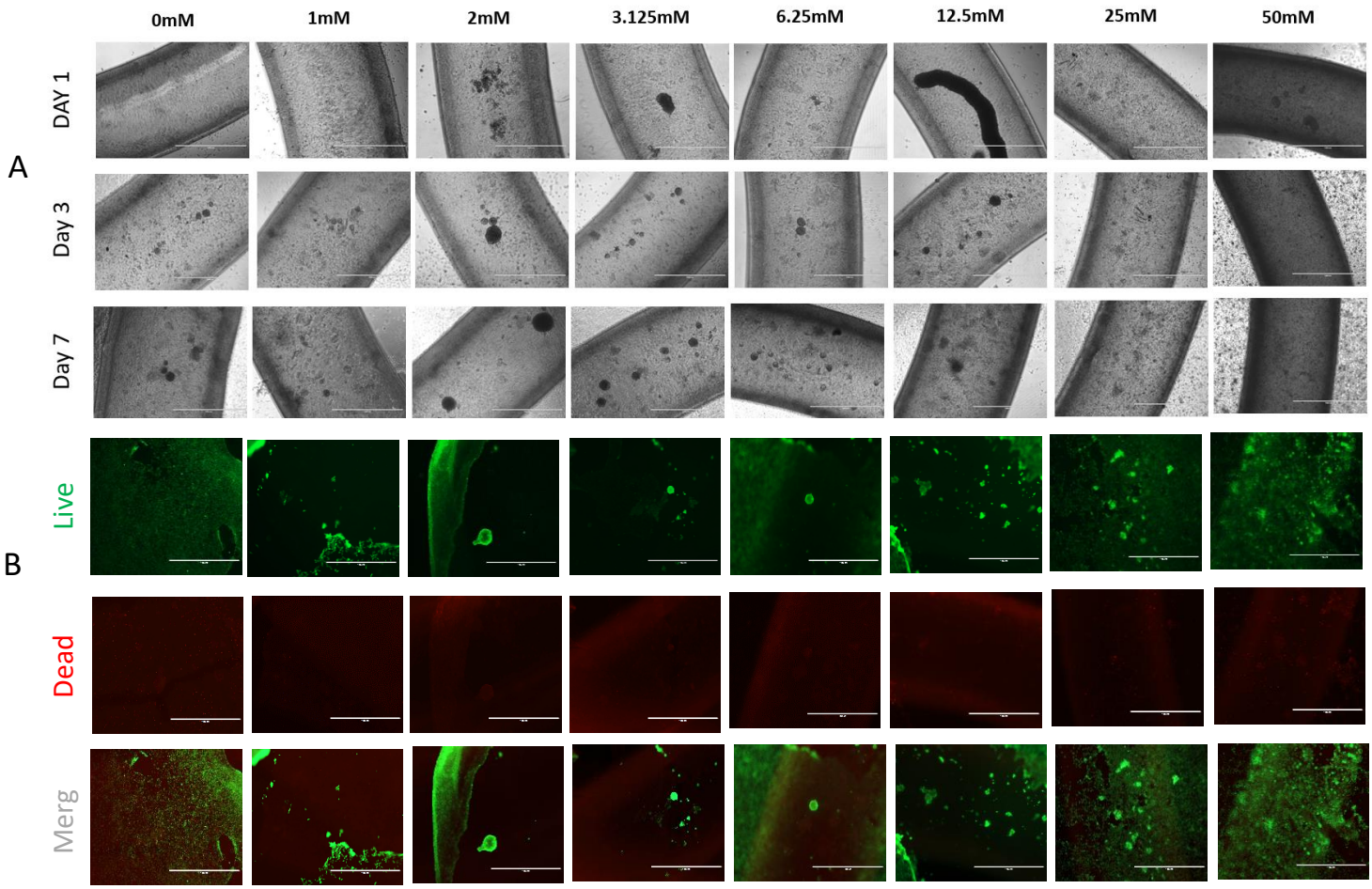

Figure 3.6. Effects of $CaCl_2$ concentration on cell morphology and viability of salivary gland epithelial SCA-9 cells grown in alginate hydrogel microtubes made of alginate at room temperature. (A) Optical Images on days 1, 3 and 7. Scale bar = 1000 um. (B) Fluorescence of Live/Dead stained cells on day 7. Green: live cells. Red: dead cells. Scale bar = 1000 µm.

found to be least effective at forming individualized and separated clusters. On day 1, there appeared to be no clusters of cells in the majority of the alginate microtubes; on day 7, only

small cell aggregates formed in microtubes when $CaCl_2$ concentration was 25 mM or below (Figure 3.6A). In the Live/Dead stain assay, most of salivary gland epithelial SCA-9 cells were alive but had escaped from the end of microtubes by day 7 (Figure 3.6B).

For the next iteration of this experiment, a co-culture of both salivary gland epithelial SCA-9 cells and NIH 3T3 fibroblasts with an epithelial to stromal ratio of 1:5 was injected into microtubes and cultured in media supplemented with 0-50 mM $CaCl_2$ as shown in figure 3.7. Cell clusters were clearly present and lined up on day 1 which appear to break apart into smaller beaded clusters on day 3. By day 7 cell clusters tended to fuse into large aggregates when co-cultured in media supplemented with 1 mM or 6.25 mM $CaCl_2$. For the rest of the $CaCl_2$ concentrations, cell clusters seemed to decrease in size on day 7 compared to day 3. The co-culture experiment had more cell clusters compared to monoculture of NIH 3T3 fibroblasts or salivary gland epithelial SCA-9 cell, suggesting that co-culture in alginate hydrogel microtubes could facilitate the stromal-epithelial cell interaction and that stromal cells may have a positive impact on salivary gland epithelial cell aggregation and cluster formation within the microtubes.

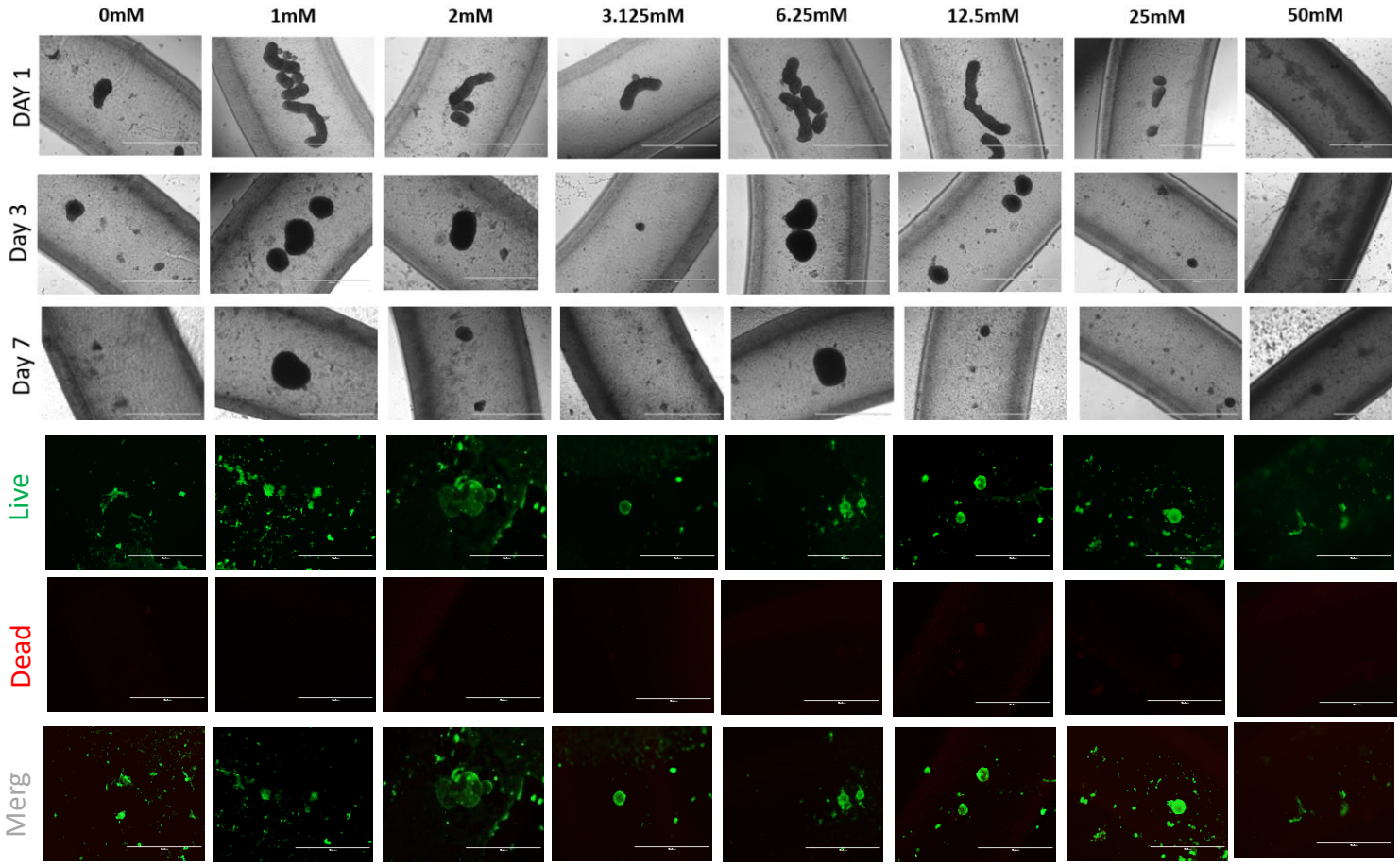

Figure 3.7. Effects of $CaCl_2$ concentration on cell morphology and viability of co-cultured salivary gland epithelial SCA-9 cells and NIH 3T3 fibroblasts at 1:5 ratio in alginate hydrogel microtubes made of alginate at room temperature. (A) Optical Images on days 1, 3 and 7. Scale bar = 1000 µm. (B) Fluorescence of Live/Dead stained cells on day 7. Green: live cells. Red: dead cells. Scale bar = 1000 µm.

3.4. Effects of low-temperature alginate on stability of microtubes and cell organization in microtubes

In experiments described in Section 3.3, the alginate solution was equilibrated to room temperature for the alginate microtube fabrication process. Medium supplemented with 12.5 mM and 25 mM $CaCl_2$ allowed cell clusters to form both when NIH 3T3 fibroblasts were cultured within the microtubes and when NIH 3T3 fibroblasts were co-cultured with salivary

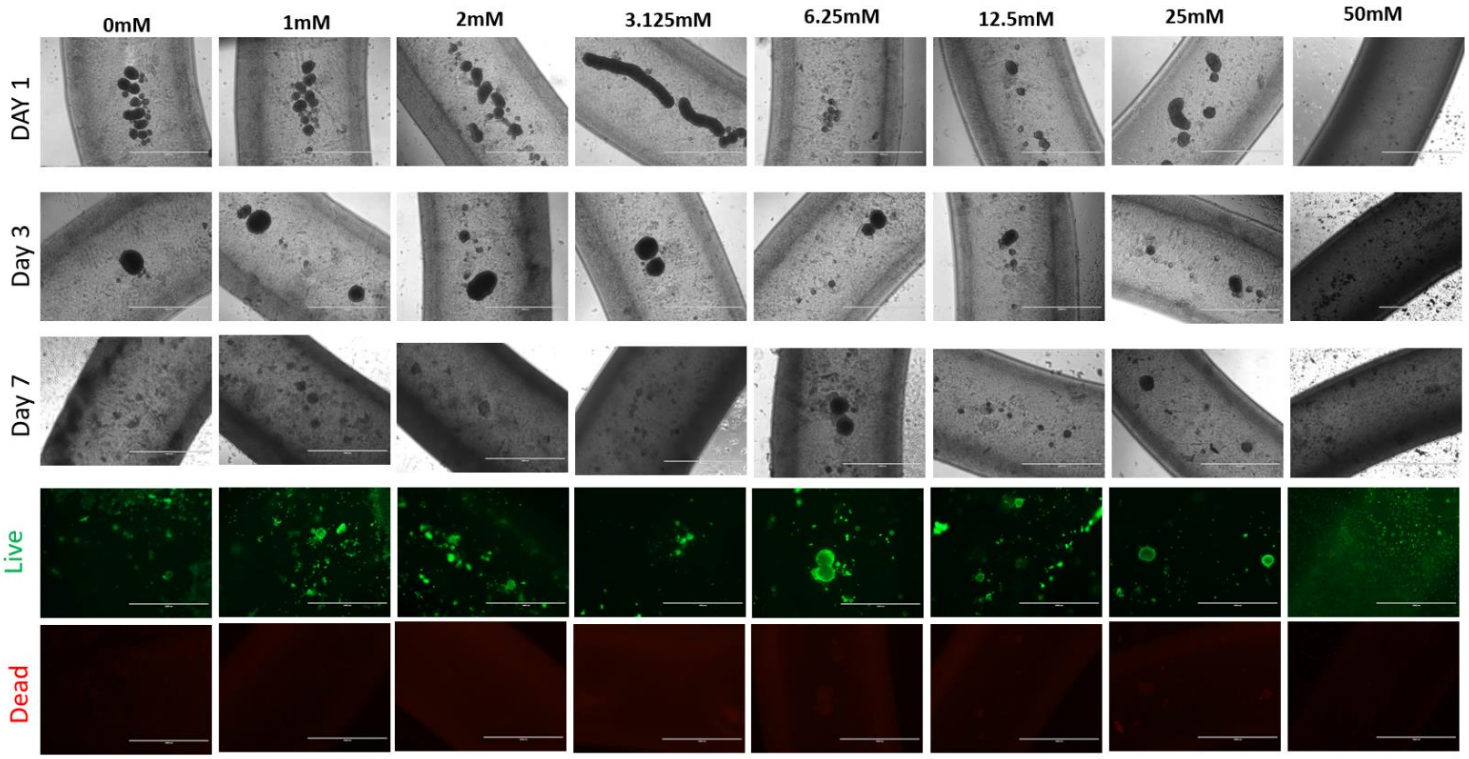

Figure 3.8. Effects of $CaCl_2$ concentration on cell morphology and viability of NIH 3T3 cells grown in alginate hydrogel microtubes made of alginate at low temperature. (A) Optical images on days 1, 3 and 7. Scale bar = 1000 μm. (B) Fluorescence of Live/Dead stained cells on day 7. Green: live cells. Red: dead cells. Scale bar = 1000 μm.

gland epithelial SCA-9 cells within the microtubes (Figure 3.4 and 3.6). However, the size of the cell clusters was not as uniform as originally expected. In order to further improve the stability and efficiency of forming uniform cell clusters in alginate hydrogel microtubes, we also

examined the effect of using alginate at 4 °C (without equilibration to room temperature) to fabricate alginate hydrogel microtubes for cell culture in media with supplemental $CaCl_2$ at different concentrations (0-50 mM). In these experiments, we used the same three sets of cell types used previously, NIH 3T3 fibroblasts alone, salivary gland epithelial SCA-9 cells alone, and co-cultured SCA-9 cells and NIH 3T3 at an epithelial to mesenchymal ratio of 1:5. We constructed the alginate microtubes using 6% sodium alginate solution at 4 °C. Cells at a density of 5.0×10^6 cells/mL were injected into these pre-made hydrogel microtubes. Cells in alginate hydrogel and microtubes were imaged on day 1, day 3, and day 7 as shown in Figure 3.8 for NIH 3T3 fibroblasts, Figure 3.9 for SCA-9 cells, and Figure 3.10 for co-cultured SCA-9 cells and NIH 3T3 fibroblasts. On day 1 we observed that differently shaped cell aggregates formed, and cells in 3.125 mM $CaCl_2$ formed rod-shaped aggregates. On day 7, most of the aggregated cells had escaped the alginate hydrogel, except for those at $CaCl_2$ concentrations of 6.25, 12.5, and 25 mM, which showed some small clusters, as shown in the optical microscope images and Live/Dead stain assay.

Next, we injected salivary gland epithelial SCA-9 cells alone into the alginate hydrogel microtube made of low temperature alginate that was stored in a refrigerator at 4 °C for 24 hours (figure 3.9) and the cell cluster formation was observed in these hydrogels on day 1, while these SCA-9 cells grown in hydrogel microtubes formed with room temperature alginate solution could not form distinct cell clusters. With an increase in $CaCl_2$ concentration, the hardness of the microtube increased, and the resilience and cohesiveness of the hydrogel increased as well, which makes these microtubes easy to handle and stable, maintaining their integrity, while keeping cell clusters inside the microtubes. As seen with room-temperature alginate solution, the SCA-9 cells the SCA-9 cells in alginate hydrogel microtubes cultured with

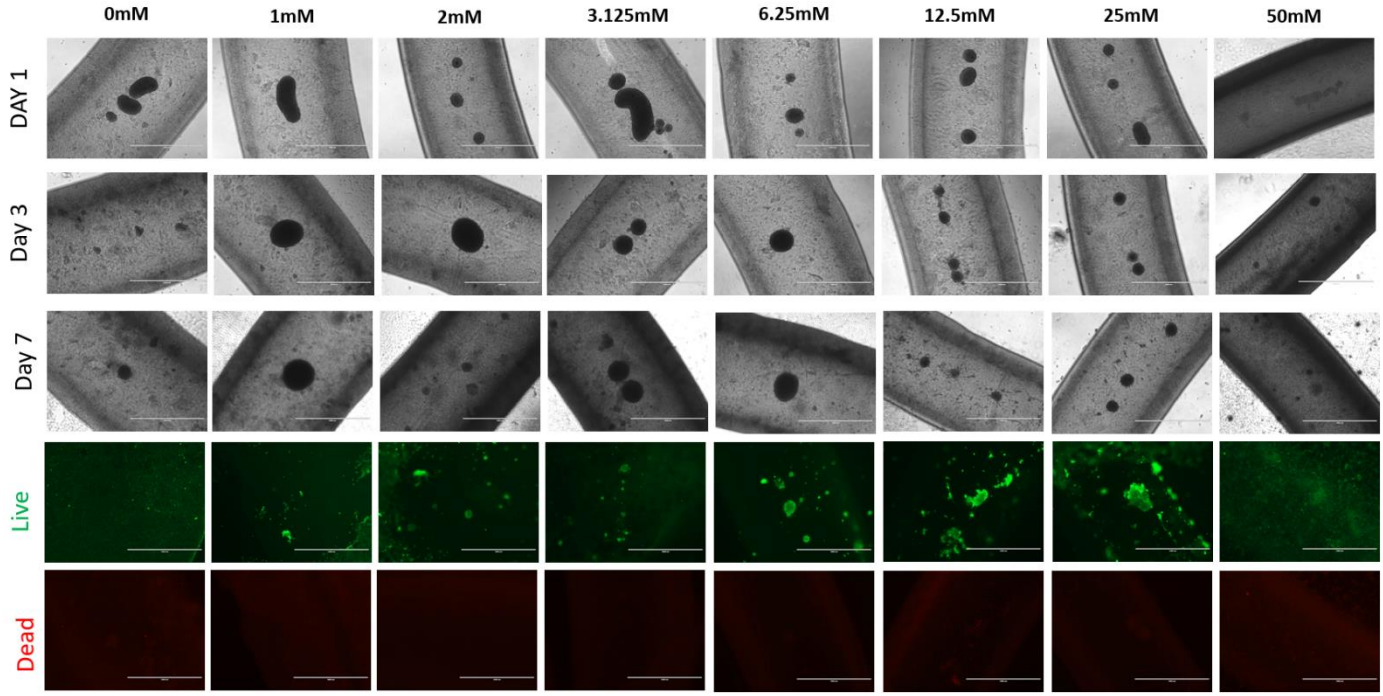

Figure 3.9. Effects of $CaCl_2$ concentration on cell morphology and viability of salivary gland epithelial SCA-9 cells grown in alginate hydrogel microtubes made of alginate at low temperature. (A) Optical Images on days 1, 3 and 7. Scale bar = 1000 µm. (B) Fluorescence of Live/Dead stained cells on day 7. Green: live cells. Red: dead cells. Scale bar = 1000 µm. Optical Images of microtube grown SCA-9 cells at low temp_ EXP#19

50 mM $CaCl_2$ showed a decrease in cell growth and cluster formation. The use of low

temperature alginate to fabricate hydrogel microtubes improved individualized and separated cell aggregation and cluster formation and the stability of the alginate microtubes. Live/Dead staining of SCA-9 cells at 6.25 mM, 12.5 mM and 25 mM $CaCl_2$ concentrations revealed viable clusters of cells. The hydrogels showed positive calcein staining, indicating that the cells were viable. Based on staining results, 6.25 mM, 12.5 mM and 25 mM appeared to have the most clusters with strong green fluorescence.

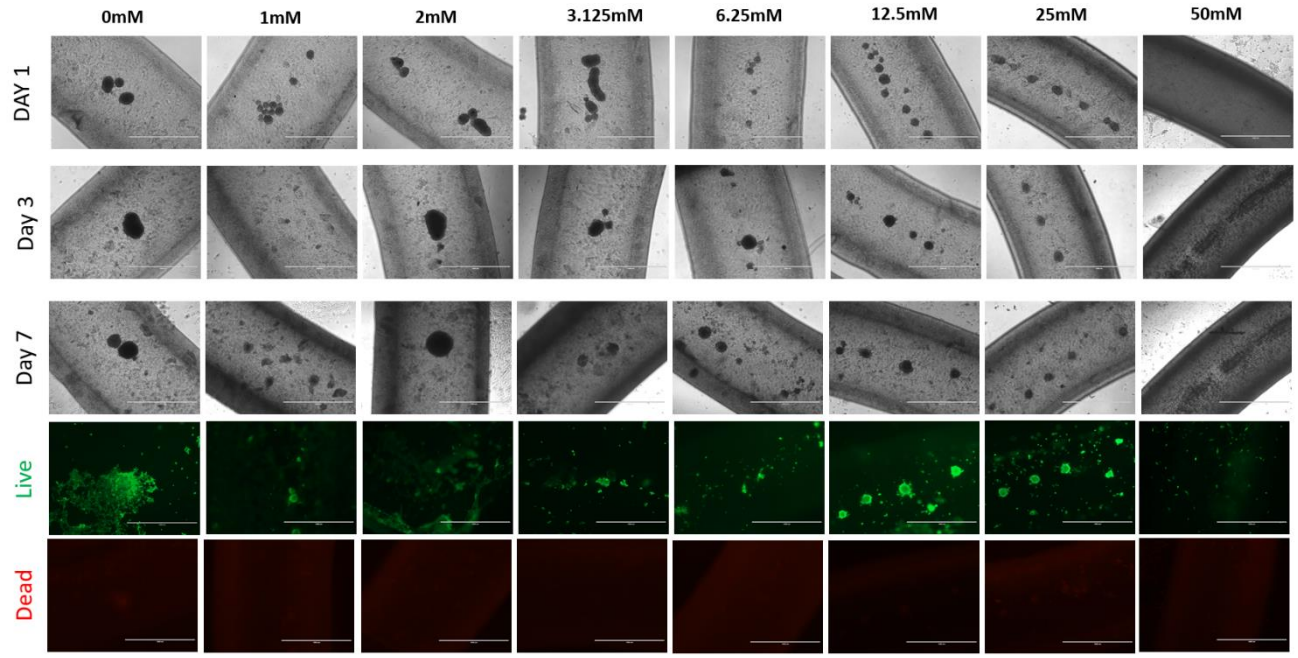

Figure 3.10. Effects of $CaCl_2$ concentration on cell morphology and viability of co-cultured salivary gland epithelial SCA-9 cells and NIH 3T3 fibroblasts at 1:5 ratio in alginate hydrogel microtubes made of alginate at low temperature. (A) Optical Images on days 1, 3 and 7. Scale bar = 1000 um. (B) Fluorescence of Live/Dead stained cells on day 7. Green: live cells. Red: dead cells. Scale bar =

The following iteration of this experiment consisted of co-culturing SCA-9 and NIH 3T3 cells in a stromal to epithelial ratio of 1:5 in hydrogel microtubes made of low-temperature alginate. In Figure 3.10, NIH 3T3 fibroblasts and salivary gland epithelial SCA-9 cells were injected into microtubes and cultured in media supplemented with $CaCl_2$ at various concentrations (0-50 mM). Among the various $CaCl_2$ concentrations tested, 12.5 mM and 25

mM promoted the most growth and were associated with the formation of small, beaded aggregates on day 1. We confirmed this correlation by reviewing the optical images and the Live/Dead staining of co-cultured cells in these microtubes on day 7. Co-cultures of NIH 3T3 and SCA-9 cells in hydrogel microtubes in the presence of 12.5 mM and 25 mM $CaCl_2$ showed the highest cell viability and uniform cell cluster formation, while the co-culture incubated in 1 mM $CaCl_2$ showed the poorest results. In the presence of 50 mM $CaCl_2$, cell growth in microtubes was poor.

This set of experiments utilized low-temperature alginate solution in the creation of hydrogel microtubes. According to the data from the previous experiments, low-temperature alginate combined with an environment supplemented with $CaCl_2$ in a concentration of 12.5

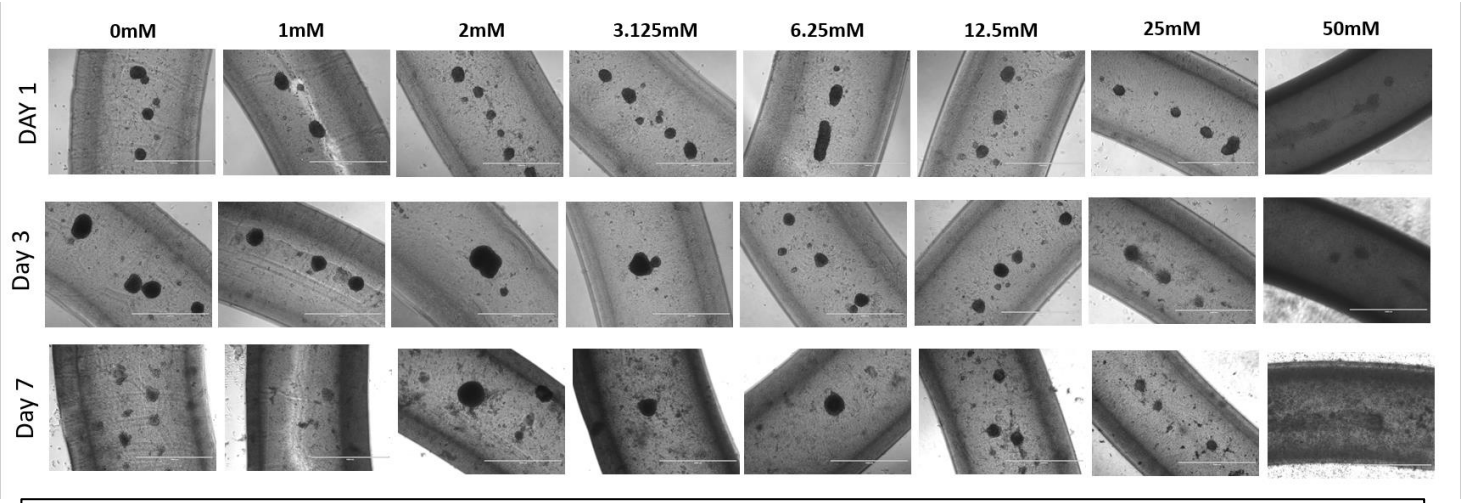

Figure 3.11. Optical images on days 1, 3, and 7 illustrating how $CaCl_2$ concentration affects cellular organization of NIH 3T3 fibroblasts and salivary gland epithelial SCA-9 cells co-cultured in hydrogel microtubes made of low-temperature alginate solution. Scale bar = 1000 um.

mM or 25 mM yields the desired results for NIH 3T3 fibroblasts alone, salivary gland epithelial SCA-9 cells alone, or co-culture of both cells. This combination yields both high structural integrity of the alginate microtubes in addition to high viability of the encapsulated cells. In order to validate this result, the co-culture experiment was repeated as shown in Figure 3.11.

This experiment confirmed that co-cultured NIH 3T3 fibroblasts and salivary gland epithelial SCA-9 cells in hydrogel microtubes made of low-temperature alginate that was stored at 4 °C for 24 hours could reproducibly generate individualized, uniform cell aggregates/clusters for 7 days in the presence of 12.5 mM or 25 mM $CaCl_2$. For short period of co-culture, such as 3 days, supplementing with 6.25 mM $CaCl_2$ allowed uniform cell cluster formation, similar to those in the presence of 12.5 and 25 mM $CaCl_2$, but tended to grow or fuse into larger aggregates after 7 days; supplementing with 2 mM or 3.125 mM $CaCl_2$, cells tended to fuse into large aggregates on day 3, but reduce size on day 7; and supplementing with 0 or 1 mM $CaCl_2$ cells tended to form uniform cell clusters on day 3, but reduce in size and appearance on day 7.

In summary, for co-culturing NIH 3T3 fibroblasts and SCA-9 cells in alginate hydrogel microtubes made of low-temperature alginate for 3 days or less, no additional $CaCl_2$ would be necessary to stabilize the microtube and enable uniform cell cluster formation. One possible reasons is that the low temperature alginate could result in a slower gelation rate (Kuo and Ma 2001) compared to room temperature and slower gelation could generate more uniform and mechanically stronger alginate hydrogels than faster gelation. Additionally, the $CaCl_2$ concentration in Dulbecco's modified Eagles medium (DMEM) is 1.8 mM, which might be sufficient to stabilize the hydrogel microtubes made from low-temperature alginate.

For longer term co-culture, such as 7 days, supplementing with 12.5 mM or 25 mM $CaCl_2$ is beneficial to improve the stability of alginate hydrogel microtubes and support reproducible, uniform cell cluster formation.

3.5. Effects of low temperature alginate on physical properties of hydrogel microtubes

As a result of the improved microtube stability and cellular organization when using low temperature alginate solution in the microtube creation process, we reopened our investigation into the impact of $CaCl_2$ on both water retention and connective porosity for microtubes made of low-temperature alginate. Alginate microtubes were created from a low-temperature alginate solution that was refrigerated in a 4 °C refrigerator for either 1 hour (Figure 3.12A) or 24 hours (Figure 3.12B) prior to microtube extrusion/fabrication. Once the elapsed time was reached, alginate microtubes were fabricated and cut into 100 mm tubes and submerged in DMEM/F12 medium supplemented with 0-50 mM $CaCl_2$ for seven days in an incubator.

The water retention was measured 7 days after incubation. We observed that when supplemental $CaCl_2$ concentration was no more than 12.5 mM, the storage of the alginate solution at 4 °C for 1 hour (1-hour-storage) or 24 hour (24-hour-storage) did not significantly affect the water retention of these microtubes, which remains at ~3.5-4%. After incubation in DMEM/F12 medium supplemented with 25 mM $CaCl_2$, the water retention rate was 6.1% for 1-hour-storage microtubes and 4.6% for 24-hour-storage microtubes. After incubation in DMEM/F12 medium supplemented with 50 mM $CaCl_2$, the water retention was 6.6% for 1-hour-storage microtubes and 7.4% for 24-hour-storage microtubes. $CaCl_2$ at higher concentrations allows for higher water retention, which is comparable to the results for alginate microtubes formed at room temperature. In fact, the graph of water retention vs. $CaCl_2$ concentration for hydrogel microtubes made of low temperature alginate stored at 4 °C for 1

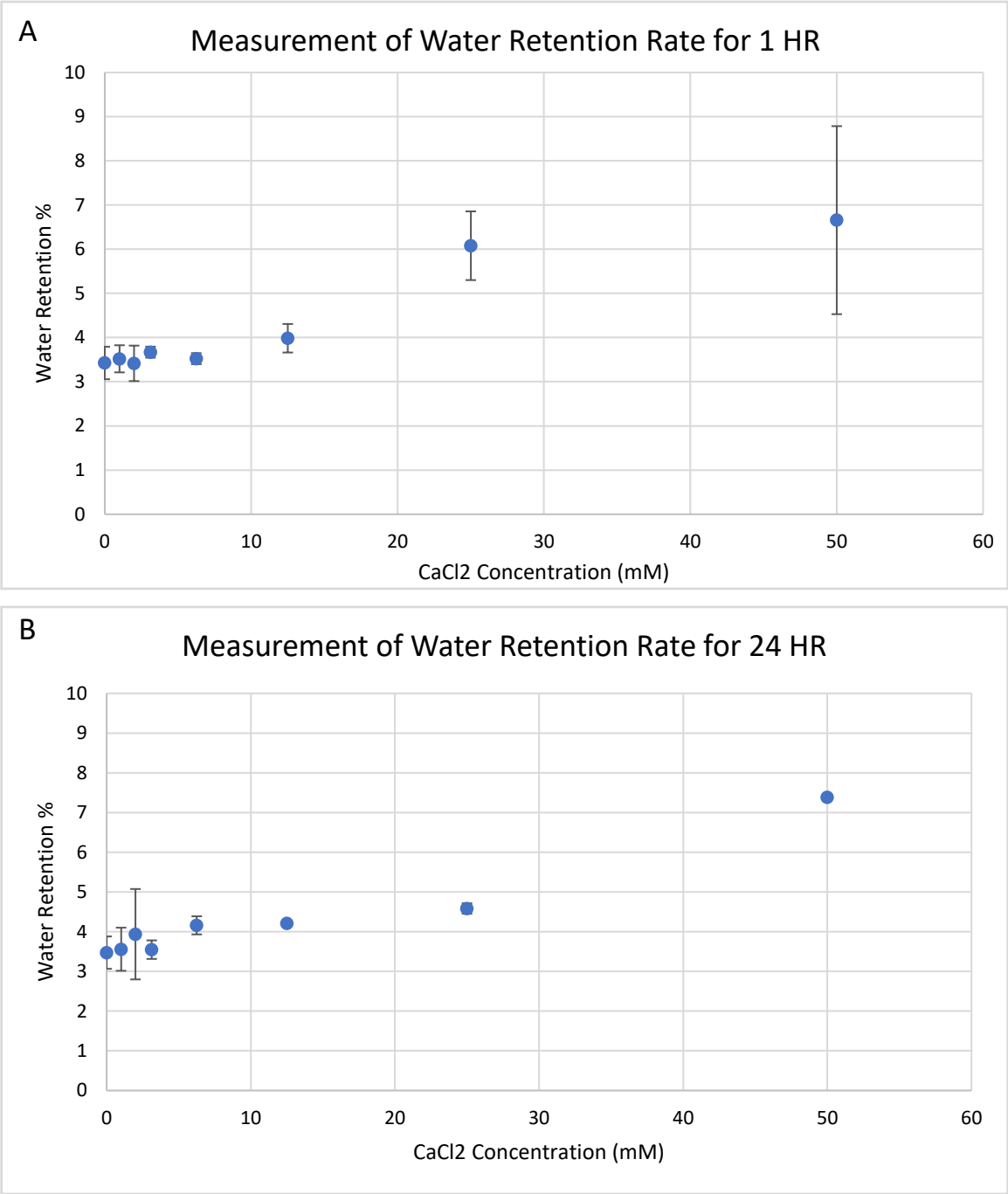

Figure 3.12. Alginate microtubes were created from low-temperature alginate solution chilled in a 4° refrigerator for either 1 hour (A) or 24 hours (B). After the elapsed time, the alginate microtubes were fabricated and cut into 100 mm microtubes and submerged in DMEM/F12 medium supplemented with a specified concentration of $CaCl_2$ in a 35 mm petri dish in an incubator for 7 days. The water retention was then measured 7 days later.

hour (Figure 3.12A) was similar to that for hydrogel microtubes made from room temperature

alginate (Figure 3.2A), implying that storage of alginate at 4 °C for 1 hour might not be enough. Interestingly, hydrogel microtubes made of alginate solution that were stored at 4 °C for 24 hours resisted significant changes in water retention when the supplemental $CaCl_2$ concentration varied from 0-25 mM.

To examine the impact of low temperature alginate solution on connective porosity, alginate microtubes were created from low-temperature alginate solution that was chilled in a 4 °C refrigerator for either 1 hour (Figure 3.13A) or 24 hours (Figure 3.13B). After the elapsed time, the alginate microtubes were fabricated and cut into 100 mm microtubes and submerged in DMEM/F12 medium supplemented with a specified concentration of $CaCl_2$ in a 35 mm petri dish in an incubator for 7 days. Seven days later, the connective porosity was measured. Similarly, to hydrogel microtubes made of room temperature alginate (Figure 3.1B), the connective porosity of these hydrogel microtubes made of low temperature alginate decreased with increased supplemental $CaCl_2$ concentration. When the alginate solution was chilled for 24 hours, the connective porosity of the resultant hydrogel microtubes appeared to be lower than that of the microtube made of alginate chilled for 1 hour after incubation with 1-25 mM $CaCl_2$, respectively. When the $CaCl_2$ concentration reached 50 mM, the connective porosity decreased to the same level (22-23%) for microtubes made of 1-hour-stored alginate and 24-hour-stored alginate. Relatively lower connective porosity indicated more crosslinking of Ca^{2+} with alginate molecules, and therefore, higher mechanical stability of alginate hydrogel microtubes. However, supplementing with 50 mM $CaCl_2$ did not support cell growth.

In summary, in order to produce alginate hydrogel microtubes for longer term culture, 6% alginate chilled at 4 °C in a refrigerator for 24 hours can be used to fabricate microtubes and 12.5 mM or 25 mM $CaCl_2$ can be supplemented to cell culture medium, which will result in microtubes with connective porosity of 35-40% and a water retention of 4-4.5%, to facilitate cell-cell interaction and support uniform cell cluster formation.

3.6. Feasibility of cell re-growth after release from alginate hydrogel microtubes

After determining the best $CaCl_2$ concentration for improving alginate microtube stability, the next goal was to determine if salivary gland stromal cells can continue to grow once they have been released from alginate hydrogel microtubes. In order to demonstrate that stromal cells could continue to grow after culturing in microtubes, mouse primary E16 mesenchyme cells isolated from submandibular salivary gland tissues were injected into alginate hydrogel microtubes and cultured in the presence of 25 mM $CaCl_2$ for seven days. On the seventh day, E16 cells were released and plated in a 24-well plate for an additional seven days to see if these cells could re-grow after being cultured in alginate hydrogel microtubes. After 7 days growth in the 24-well plates, cells were stained for the mesenchymal marker, vimentin, to see if cell phenotype was also retained.

After mouse primary E16 mesenchymal cells were released from alginate microtubes and replated, optical images were taken to show the growth of these cells and their progress on days 1, 4, and 7. The progress of the cell growth was clear as these cells continued to grow and reach confluence on the 7^{th} day. The confocal images confirmed characteristic expression of vimentin, a mesenchymal marker, co-stained with DAPI to show the nuclei of

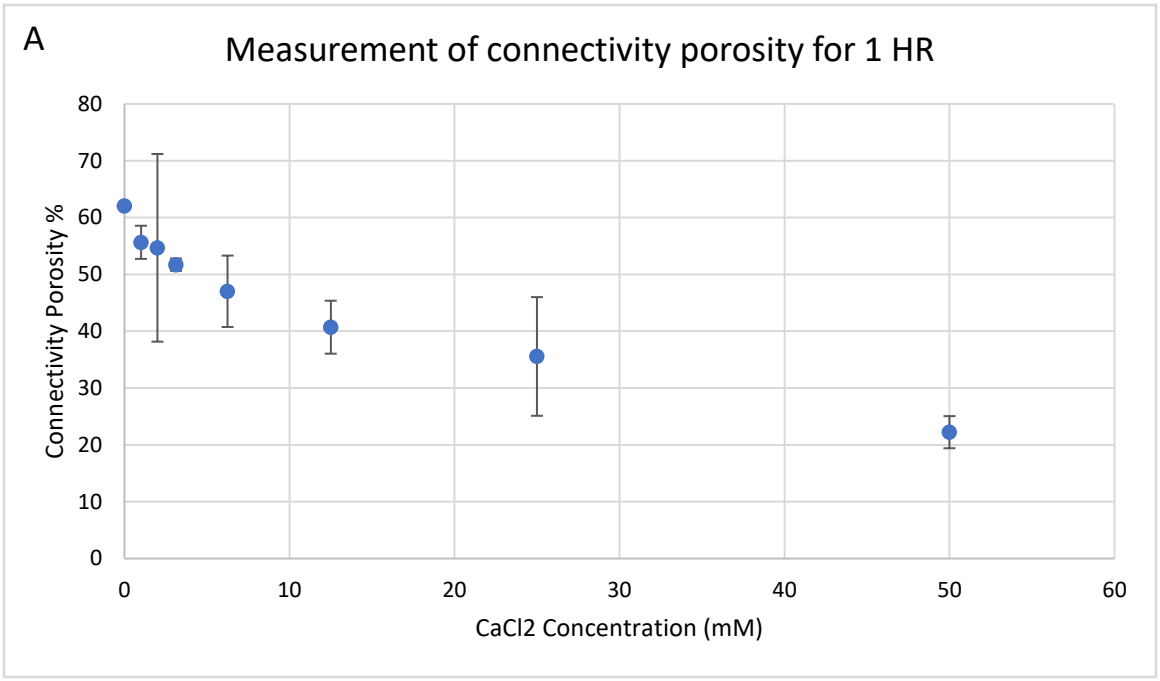

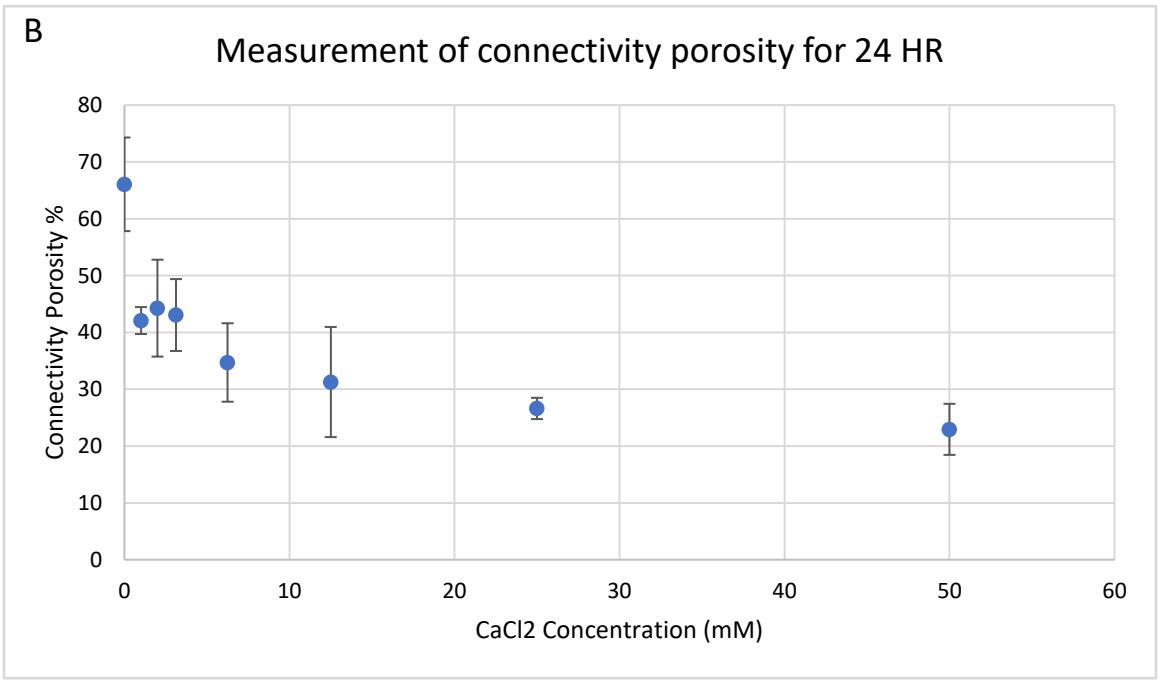

Figure 3.13. Alginate microtubes were created from low-temperature alginate solution chilled in a 4°C refrigerator for either 1 hour (A) or 24 hours (B). After the elapsed time, the alginate microtubes were fabricated and cut into 100 mm microtubes and submerged in DMEM/F12 media supplemented with a specified concentration of $CaCl_2$ in a 35 mm petri dish in an incubator for 7 days. Connective porosity was then measured 7 days later.

total cell population on the 7th day. These results continue to validate the usefulness of alginate microtubes for cell expansion and maintenance since the cells retain the ability to proliferate and express their characteristic markers after release from the alginate hydrogel microtubes being cultured, even in the presence of 25 mM $CaCl_2$.

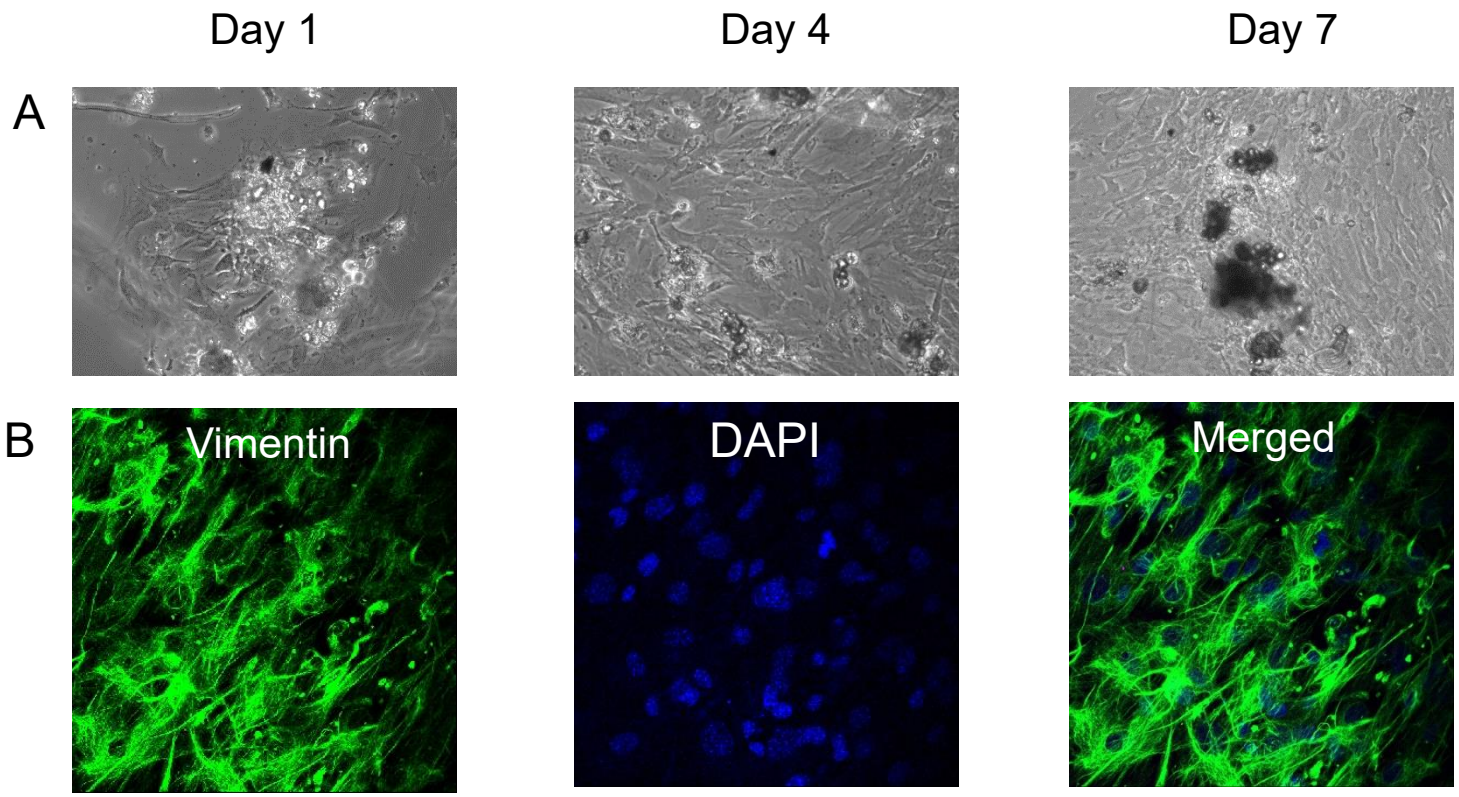

Figure 3.14 Images of primary E16 mesenchyme cells re-plated in a 6-well plate showing that these cells could re-grow after culturing in alginate hydrogel microtubes for 7 days followed by releasing cells from the microtube. (a) Optical images showing cell growth on days 1, 4 and 7. (Magnification: 20×) (b) Confocal images showing expression of vimentin after re-growing in a 6-well plate for 7 days. (Green: vimentin; Purple: DAPI-stained nuclei, Magnification: 63×).

Chapter 4 Conclusions and Future Directions

4.1. Conclusions

To study cells and complex organs that naturally form in vivo as accurately and reliably as possible, it is imperative to mimic the native microenvironment of the region of interest. Using alginate hydrogels for the functional engineering of soft tissues provides a useful option for 3D scaffolding and culture due to all the benefits illustrated previously, such as their natural biocompatibility, biodegradability, porous structure, and tunable physical properties, all of which make alginate hydrogels a compliant microenvironment for cell migration, interaction, and organization. The ability to recreate the 3D microenvironment allows greater insight into cells' in vivo interactions and behavior while using an in vitro platform. There are, however, significant challenges associated with engineering soft tissues in 3D, primarily due to the complexity of engineered alginate hydrogels as well as their instability when phosphate is present in the cell culture media.

Previous work in our lab included developing techniques for producing structurally uniform alginate hydrogel microtubes by using a needle-in-needle device to mix 6% sodium alginate with 100 mM $CaCl_2$. However, the stability of alginate hydrogel tended to decrease during 7-day culture due to the presence of phosphate in the media. Our current study aimed to determine the optimal $CaCl_2$ concentration to be added to the cell culture medium for stabilization of alginate hydrogel. We also wanted to determine whether cells continue to grow once released from microtubes. This study was carried out by varying the concentration of $CaCl_2$ in the cell culture medium between 1 mM and 50 mM, using cell culture without $CaCl_2$ supplementation as the control to find the most effective $CaCl_2$ concentration for cell culture in

alginate hydrogel microtubes. Our research investigated the impact of $CaCl_2$ on the physical properties of the alginate hydrogel microtubes and cell growth. We aim to reveal the optimal $CaCl_2$ concentration supplementation that would create stability and preserve the mechanical properties of ionically crosslinked hydrogels in a tissue culture environment (an aqueous medium). Since $CaCl_2$ concentration is known to affect the porous structure and the swelling characteristics of alginate microtubes, the connective porosity and water retention of our alginate microtubes were studied after supplementation with different concentrations of $CaCl_2$.

Our findings allow us to conclude that as the $CaCl_2$ concentration was increased from 1 mM to 50 mM, the water retention of the alginate hydrogel microtubes generally increased. In our study of the connective porosity, we found that as $CaCl_2$ concentration increased, the connective porosity decreased. Our results show that supplementation with $CaCl_2$ reduced connective porosity, which could increase the structure stability of hydrogel, and improve water retention of alginate hydrogel microtubes, which would create a better aqueous 3D microenvironment for cell culture.

To study the impact of $CaCl_2$ concentration on cell viability and organization, stromal cells and salivary gland epithelial cells were injected into our alginate hydrogel microtubes for monocultures and co-culture, respectively. In particular, we found that using 6% alginate solution chilled at 4 °C for 24 hours, we could fabricate hydrogel microtubes that were stable and support cell cluster formation for 3 days even in the absence of supplemental $CaCl_2$. For longer-term culture, such as 7 days, $CaCl_2$ concentration was found to impact cell cluster formation with the ideal $CaCl_2$ concentration for consistent, uniform cluster formation being 12.5 and 25 mM. While $CaCl_2$ has an impact on the cells being incubated, the desired use is for

our ability to prevent the degradation of our alginate hydrogel microtubes. When we studied varying the $CaCl_2$ concentration on hydrogel microtubes after 7 days of incubation it was found that 12.5 and 25 mM again provided a good environment for our hydrogel microtubes to maintain their physical properties. Through our observations, we have been able to validate that cells can survive when encapsulated in the hydrogel alginate microtubes. In addition, they retain the capacity for continued growth once released from the microtubes. Through our experiments, we have observed that a 25 mM concentration of $CaCl_2$ is appropriate and acts as a "Goldi-locks" level since it is high enough to protect the physical integrity of the alginate microtubes while not being so high that negative consequences become apparent for growing cells.

In summary, we have demonstrated a method to control the mechanical properties of our unique alginate microtubes strengthen their stability as a scaffold for salivary gland stromal and epithelial cell growth. In addition, we have validated that our hydrogel microtube platform is capable of functioning as a platform for stimulating formation of 3D cell spheroids that may behave in a manner similar to how cells behave in vivo, without negatively affecting their ability to grow and proliferate when released from the 3D matrix.

4.2. Future Directions

In the future, we will examine the growth and organization of cells grown and released from alginate hydrogel microtubes over a longer period. Cell type appears to play an important role in cluster formation. Further studies can be done on the interaction between cells and how

our alginate microtubes might be tuned in the future to allow or even amplify desired cell signaling.

References

A, S., As, V., & D, V. (2019). Porous Alginate Scaffolds Assembled Using Vaterite CaCO 3 Crystals. *Micromachines*, *10*(6). https://doi.org/10.3390/mi10060357

Aderibigbe, B. A., & Buyana, B. (2018). Alginate in Wound Dressings. *Pharmaceutics*, *10*(2), E42. https://doi.org/10.3390/pharmaceutics10020042

Afewerki, S., Sheikhi, A., Kannan, S., Ahadian, S., & Khademhosseini, A. (2019). Gelatin-polysaccharide composite scaffolds for 3D cell culture and tissue engineering: Towards natural therapeutics. *Bioengineering & Translational Medicine*, *4*(1), 96–115. https://doi.org/10.1002/btm2.10124

Alsberg, E., Anderson, K. W., Albeiruti, A., Rowley, J. A., & Mooney, D. J. (2002). Engineering growing tissues. *Proceedings of the National Academy of Sciences of the United States of America*, *99*(19), 12025–12030. https://doi.org/10.1073/pnas.192291499

Annabi, N., Tamayol, A., Uquillas, J. A., Akbari, M., Bertassoni, L. E., Cha, C., Camci-Unal, G., Dokmeci, M. R., Peppas, N. A., & Khademhosseini, A. (2014). 25th anniversary article: Rational design and applications of hydrogels in regenerative medicine. *Advanced Materials (Deerfield Beach, Fla.)*, *26*(1), 85–123. https://doi.org/10.1002/adma.201303233

Atkinson, J. C., Grisius, M., & Massey, W. (2005). Salivary hypofunction and xerostomia: Diagnosis and treatment. *Dental Clinics of North America*, *49*(2), 309–326. https://doi.org/10.1016/j.cden.2004.10.002

Augst, A. D., Kong, H. J., & Mooney, D. J. (2006). Alginate hydrogels as biomaterials. *Macromolecular Bioscience*, *6*(8), 623–633. https://doi.org/10.1002/mabi.200600069

Bao, M., Xie, J., & Huck, W. T. S. (2018a). Recent Advances in Engineering the Stem Cell Microniche in 3D. *Advanced Science (Weinheim, Baden-Wurttemberg, Germany)*, *5*(8), 1800448. https://doi.org/10.1002/advs.201800448

Bao, M., Xie, J., & Huck, W. T. S. (2018b). Recent Advances in Engineering the Stem Cell Microniche in 3D. *Advanced Science (Weinheim, Baden-Wurttemberg, Germany)*, *5*(8), 1800448. https://doi.org/10.1002/advs.201800448

Barrows, C. M. L., Wu, D., Farach-Carson, M. C., & Young, S. (2020). Building a Functional Salivary Gland for Cell-Based Therapy: More than Secretory Epithelial Acini. *Tissue Engineering. Part A*, *26*(23–24), 1332–1348. https://doi.org/10.1089/ten.TEA.2020.0184

Bhide, S. A., Miah, A. B., Harrington, K. J., Newbold, K. L., & Nutting, C. M. (2009). Radiation-induced xerostomia: Pathophysiology, prevention and treatment. *Clinical Oncology (Royal College of Radiologists (Great Britain))*, *21*(10), 737–744. https://doi.org/10.1016/j.clon.2009.09.002

Cantara, S. I., Soscia, D. A., Sequeira, S., Jean-Gilles, R., Castracane, J., & Larsen, M. (2012). Selective functionalization of nanofiber scaffolds to regulate salivary gland epithelial cell proliferation and polarity. *Biomaterials*, *33*(33), 8372–8382. https://doi.org/10.1016/j.biomaterials.2012.08.021

Ching, S. H., Bansal, N., & Bhandari, B. (2017). Alginate gel particles-A review of production techniques and physical properties. *Critical Reviews in Food Science and Nutrition*, *57*(6), 1133–1152. https://doi.org/10.1080/10408398.2014.965773

Chu, J., Zeng, S., Gao, L., Groth, T., Li, Z., Kong, J., Zhao, M., & Li, L. (2016). Poly (L-lactic acid) porous scaffold-supported alginate hydrogel with improved mechanical properties and biocompatibility. *The International Journal of Artificial Organs*, *39*(8), 435–443. https://doi.org/10.5301/ijao.5000516

Discher, D. E., Janmey, P., & Wang, Y.-L. (2005). Tissue cells feel and respond to the stiffness of their substrate. *Science (New York, N.Y.)*, *310*(5751), 1139–1143. https://doi.org/10.1126/science.1116995

Fontoura, J. C., Viezzer, C., Dos Santos, F. G., Ligabue, R. A., Weinlich, R., Puga, R. D., Antonow, D., Severino, P., & Bonorino, C. (2020). Comparison of 2D and 3D cell culture models for cell growth, gene expression

and drug resistance. *Materials Science & Engineering. C, Materials for Biological Applications*, *107*, 110264. https://doi.org/10.1016/j.msec.2019.110264

Foraida, Z. I., Kamaldinov, T., Nelson, D. A., Larsen, M., & Castracane, J. (2017). Elastin-PLGA hybrid electrospun nanofiber scaffolds for salivary epithelial cell self-organization and polarization. *Acta Biomaterialia*, *62*, 116–127. https://doi.org/10.1016/j.actbio.2017.08.009

Foraida, Z. I., Sharikova, A., Peerzada, L. N., Khmaladze, A., Larsen, M., & Castracane, J. (2017). Double emulsion electrospun nanofibers as a growth factor delivery vehicle for salivary gland regeneration. *Biosensing and Nanomedicine X*, *10352*, 21–29. https://doi.org/10.1117/12.2275489

Gao, J., Yu, X., Wang, X., He, Y., & Ding, J. (2022). Biomaterial–Related Cell Microenvironment in Tissue Engineering and Regenerative Medicine. *Engineering*, *13*, 31–45. https://doi.org/10.1016/j.eng.2021.11.025

Grant, G. T., Morris, E. R., Rees, D. A., Smith, P. J. C., & Thom, D. (1973). Biological interactions between polysaccharides and divalent cations: The egg-box model. *FEBS Letters*, *32*(1), 195–198. https://doi.org/10.1016/0014-5793(73)80770-7

Green, J. J., & Elisseeff, J. H. (2016). Mimicking biological functionality with polymers for biomedical applications. *Nature*, *540*(7633), 386–394. https://doi.org/10.1038/nature21005

Griffith, L. G., & Naughton, G. (2002). Tissue engineering—Current challenges and expanding opportunities. *Science (New York, N.Y.)*, *295*(5557), 1009–1014. https://doi.org/10.1126/science.1069210

Griffith, L. G., & Swartz, M. A. (2006). Capturing complex 3D tissue physiology in vitro. *Nature Reviews. Molecular Cell Biology*, *7*(3), 211–224. https://doi.org/10.1038/nrm1858

Grijalvo, S., Nieto-Díaz, M., Maza, R. M., Eritja, R., & Díaz, D. D. (2019). Alginate Hydrogels as Scaffolds and Delivery Systems to Repair the Damaged Spinal Cord. *Biotechnology Journal*, *14*(12), e1900275. https://doi.org/10.1002/biot.201900275

Hofer, M., & Lutolf, M. P. (2021). Engineering organoids. *Nature Reviews. Materials*, *6*(5), 402–420. https://doi.org/10.1038/s41578-021-00279-y

Hosseini, Z. F., Nelson, D. A., Moskwa, N., Sfakis, L. M., Castracane, J., & Larsen, M. (2018). FGF2-dependent mesenchyme and laminin-111 are niche factors in salivary gland organoids. *Journal of Cell Science*, *131*(4), jcs208728. https://doi.org/10.1242/jcs.208728

Humphrey, S. P., & Williamson, R. T. (2001). A review of saliva: Normal composition, flow, and function. *The Journal of Prosthetic Dentistry*, *85*(2), 162–169. https://doi.org/10.1067/mpr.2001.113778

Hunt, N. C., Smith, A. M., Gbureck, U., Shelton, R. M., & Grover, L. M. (2010). Encapsulation of fibroblasts causes accelerated alginate hydrogel degradation. *Acta Biomaterialia*, *6*(9), 3649–3656. https://doi.org/10.1016/j.actbio.2010.03.026

Jean-Gilles, R., Soscia, D., Sequeira, S., Melfi, M., Gadre, A., Castracane, J., & Larsen, M. (2010). Novel Modeling Approach to Generate a Polymeric Nanofiber Scaffold for Salivary Gland Cells. *Journal of Nanotechnology in Engineering and Medicine*, *1*(3), 031008. https://doi.org/10.1115/1.4001744

Jiao, W., Li, X., Shan, J., & Wang, X. (2022). Study of Several Alginate-Based Hydrogels for In Vitro 3D Cell Cultures. *Gels (Basel, Switzerland)*, *8*(3), 147. https://doi.org/10.3390/gels8030147

Jorgensen, M., Gibbons, A., Sui, K., Carpenter, R., Zhang, X., & Xie, Y. (2021). Predictable fabrication of pre-made alginate hydrogel microtubes for stem cell aggregation using needle-in-needle devices. *Biofabrication*, *13*(3). https://doi.org/10.1088/1758-5090/abfd7b

Jorgensen, M., Ramesh, P., Toro, M., Evans, E., Moskwa, N., Zhang, X., Sharfstein, S. T., Larsen, M., & Xie, Y. (2022). Alginate Hydrogel Microtubes for Salivary Gland Cell Organization and Cavitation. *Bioengineering (Basel, Switzerland)*, *9*(1), 38. https://doi.org/10.3390/bioengineering9010038

Jun, Y., Kim, M. J., Hwang, Y. H., Jeon, E. A., Kang, A. R., Lee, S.-H., & Lee, D. Y. (2013). Microfluidics-generated pancreatic islet microfibers for enhanced immunoprotection. *Biomaterials*, *34*(33), 8122–8130. https://doi.org/10.1016/j.biomaterials.2013.07.079

Kagami, H., Wang, S., & Hai, B. (2008). Restoring the function of salivary glands. *Oral Diseases*, *14*(1), 15–24. https://doi.org/10.1111/j.1601-0825.2006.01339.x

Khalil, A. S., Jaenisch, R., & Mooney, D. J. (2020). Engineered tissues and strategies to overcome challenges in drug development. *Advanced Drug Delivery Reviews*, *158*, 116–139. https://doi.org/10.1016/j.addr.2020.09.012

Koslow, M., O'Keefe, K. J., Hosseini, Z. F., Nelson, D. A., & Larsen, M. (2019). ROCK inhibitor increases proacinar cells in adult salivary gland organoids. *Stem Cell Research*, *41*, 101608. https://doi.org/10.1016/j.scr.2019.101608

Kuo, C. K., & Ma, P. X. (2001). Ionically crosslinked alginate hydrogels as scaffolds for tissue engineering: Part 1. Structure, gelation rate and mechanical properties. *Biomaterials*, *22*(6), 511–521. https://doi.org/10.1016/s0142-9612(00)00201-5

Langer, R., & Vacanti, J. (2016). Advances in tissue engineering. *Journal of Pediatric Surgery*, *51*(1), 8–12. https://doi.org/10.1016/j.jpedsurg.2015.10.022

Langer, R., & Vacanti, J. P. (1993). Tissue engineering. *Science (New York, N.Y.)*, *260*(5110), 920–926. https://doi.org/10.1126/science.8493529

Lawrence, B. J., & Madihally, S. V. (2008). Cell colonization in degradable 3D porous matrices. *Cell Adhesion & Migration*, *2*(1), 9–16. https://doi.org/10.4161/cam.2.1.5884

Lee, K. Y., & Mooney, D. J. (2001). Hydrogels for tissue engineering. *Chemical Reviews*, *101*(7), 1869–1879. https://doi.org/10.1021/cr000108x

Lee, K. Y., & Mooney, D. J. (2012). Alginate: Properties and biomedical applications. *Progress in Polymer Science*, *37*(1), 106–126. https://doi.org/10.1016/j.progpolymsci.2011.06.003

Li, L., Yu, F., Zheng, L., Wang, R., Yan, W., Wang, Z., Xu, J., Wu, J., Shi, D., Zhu, L., Wang, X., & Jiang, Q. (2019a). Natural hydrogels for cartilage regeneration: Modification, preparation and application. *Journal of Orthopaedic Translation*, *17*, 26–41. https://doi.org/10.1016/j.jot.2018.09.003

Li, L., Yu, F., Zheng, L., Wang, R., Yan, W., Wang, Z., Xu, J., Wu, J., Shi, D., Zhu, L., Wang, X., & Jiang, Q. (2019b). Natural hydrogels for cartilage regeneration: Modification, preparation and application. *Journal of Orthopaedic Translation*, *17*, 26–41. https://doi.org/10.1016/j.jot.2018.09.003

Li, Q., Lin, H., Du, Q., Liu, K., Wang, O., Evans, C., Christian, H., Zhang, C., & Lei, Y. (2018). Scalable and physiologically relevant microenvironments for human pluripotent stem cell expansion and differentiation. *Biofabrication*, *10*(2), 025006. https://doi.org/10.1088/1758-5090/aaa6b5

Li, Q., Lin, H., Rauch, J., Deleyrolle, L. P., Reynolds, B. A., Viljoen, H. J., Zhang, C., Zhang, C., Gu, L., Van Wyk, E., & Lei, Y. (2018). Scalable Culturing of Primary Human Glioblastoma Tumor-Initiating Cells with a Cell-Friendly Culture System. *Scientific Reports*, *8*, 3531. https://doi.org/10.1038/s41598-018-21927-4

Lin, H., Du, Q., Li, Q., Wang, O., Wang, Z., Liu, K., Elowsky, C., Zhang, C., & Lei, Y. (2018). Hydrogel-Based Bioprocess for Scalable Manufacturing of Human Pluripotent Stem Cell-Derived Neural Stem Cells. *ACS Applied Materials & Interfaces*, *10*(35), 29238–29250. https://doi.org/10.1021/acsami.8b05780

Lin, H., Li, Q., Wang, O., Rauch, J., Harm, B., Viljoen, H. J., Zhang, C., Van Wyk, E., Zhang, C., & Lei, Y. (2018). Automated Expansion of Primary Human T Cells in Scalable and Cell-Friendly Hydrogel Microtubes for Adoptive Immunotherapy. *Advanced Healthcare Materials*, *7*(15), e1701297. https://doi.org/10.1002/adhm.201701297

Lin, H., Qiu, X., Du, Q., Li, Q., Wang, O., Akert, L., Wang, Z., Anderson, D., Liu, K., Gu, L., Zhang, C., & Lei, Y. (2018). Engineered Microenvironment for Manufacturing Human Pluripotent Stem Cell-Derived Vascular Smooth Muscle Cells. *Stem Cell Reports*, *12*(1), 84–97. https://doi.org/10.1016/j.stemcr.2018.11.009

Liu, M., Zhou, Z., Chai, Y., Zhang, S., Wu, X., Huang, S., Su, J., & Jiang, J. (2017). Synthesis of cell composite alginate microfibers by microfluidics with the application potential of small diameter vascular grafts. *Biofabrication*, *9*(2), 025030. https://doi.org/10.1088/1758-5090/aa71da

Lutolf, M. P., Gilbert, P. M., & Blau, H. M. (2009). Designing materials to direct stem-cell fate. *Nature*, *462*(7272), 433–441. https://doi.org/10.1038/nature08602

Lutolf, M. P., & Hubbell, J. A. (2005). Synthetic biomaterials as instructive extracellular microenvironments for morphogenesis in tissue engineering. *Nature Biotechnology*, *23*(1), 47–55. https://doi.org/10.1038/nbt1055

Maria, O. M., Zeitouni, A., Gologan, O., & Tran, S. D. (2011). Matrigel improves functional properties of primary human salivary gland cells. *Tissue Engineering. Part A*, *17*(9–10), 1229–1238. https://doi.org/10.1089/ten.TEA.2010.0297

McNamara, M. C., Sharifi, F., Wrede, A. H., Kimlinger, D. F., Thomas, D.-G., Vander Wiel, J. B., Chen, Y., Montazami, R., & Hashemi, N. N. (2017). Microfibers as Physiologically Relevant Platforms for Creation of 3D Cell Cultures. *Macromolecular Bioscience*, *17*(12). https://doi.org/10.1002/mabi.201700279

Mørch, Y. A., Donati, I., Strand, B. L., & Skjåk-Braek, G. (2006). Effect of Ca2+, Ba2+, and Sr2+ on alginate microbeads. *Biomacromolecules*, *7*(5), 1471–1480. https://doi.org/10.1021/bm060010d

Nagata, S., Ozawa, F., Nie, M., & Takeuchi, S. (2020). 3D culture of functional human iPSC-derived hepatocytes using a core-shell microfiber. *PLoS ONE*, *15*(6), e0234441. https://doi.org/10.1371/journal.pone.0234441

Namgung, B., Ravi, K., Vikraman, P. P., Sengupta, S., & Jang, H. L. (2021). Engineered cell-laden alginate microparticles for 3D culture. *Biochemical Society Transactions*, *49*(2), 761–773. https://doi.org/10.1042/BST20200673

Ogawa, M., & Tsuji, T. (2015). Functional salivary gland regeneration as the next generation of organ replacement regenerative therapy. *Odontology*, *103*(3), 248–257. https://doi.org/10.1007/s10266-015-0210-9

Olmsted, Z. T., Stigliano, C., Badri, A., Zhang, F., Williams, A., Koffas, M. A. G., Xie, Y., Linhardt, R. J., Cibelli, J., Horner, P. J., & Paluh, J. L. (2020). Fabrication of homotypic neural ribbons as a multiplex platform optimized for spinal cord delivery. *Scientific Reports*, *10*(1), 12939. https://doi.org/10.1038/s41598-020-69274-7

Onoe, H., Okitsu, T., Itou, A., Kato-Negishi, M., Gojo, R., Kiriya, D., Sato, K., Miura, S., Iwanaga, S., Kuribayashi-Shigetomi, K., Matsunaga, Y. T., Shimoyama, Y., & Takeuchi, S. (2013). Metre-long cell-laden microfibres exhibit tissue morphologies and functions. *Nature Materials*, *12*(6), 584–590. https://doi.org/10.1038/nmat3606

Peters, S. B., Naim, N., Nelson, D. A., Mosier, A. P., Cady, N. C., & Larsen, M. (2014). Biocompatible tissue scaffold compliance promotes salivary gland morphogenesis and differentiation. *Tissue Engineering. Part A*, *20*(11–12), 1632–1642. https://doi.org/10.1089/ten.TEA.2013.0515

Place, E. S., George, J. H., Williams, C. K., & Stevens, M. M. (2009). Synthetic polymer scaffolds for tissue engineering. *Chemical Society Reviews*, *38*(4), 1139–1151. https://doi.org/10.1039/b811392k

Poon, C. (2022). Measuring the density and viscosity of culture media for optimized computational fluid dynamics analysis of in vitro devices. *Journal of the Mechanical Behavior of Biomedical Materials*, *126*, 105024. https://doi.org/10.1016/j.jmbbm.2021.105024

Ramesh, P., Moskwa, N., Hanchon, Z., Koplas, A., Nelson, D. A., Mills, K. L., Castracane, J., Larsen, M., Sharfstein, S. T., & Xie, Y. (2022). Engineering cryoelectrospun elastin-alginate scaffolds to serve as stromal extracellular matrices. *Biofabrication*, *14*(3). https://doi.org/10.1088/1758-5090/ac6b34

Raus, R. A., Nawawi, W. M. F. W., & Nasaruddin, R. R. (2021). Alginate and alginate composites for biomedical applications. *Asian Journal of Pharmaceutical Sciences*, *16*(3), 280. https://doi.org/10.1016/j.ajps.2020.10.001

Razavi, M., Qiao, Y., & Thakor, A. S. (2019). Three-dimensional cryogels for biomedical applications. *Journal of Biomedical Materials Research. Part A*, *107*(12), 2736–2755. https://doi.org/10.1002/jbm.a.36777

Rowley, J. A., Madlambayan, G., & Mooney, D. J. (1999). Alginate hydrogels as synthetic extracellular matrix materials. *Biomaterials*, *20*(1), 45–53. https://doi.org/10.1016/s0142-9612(98)00107-0

Sequeira, S. J., Soscia, D. A., Oztan, B., Mosier, A. P., Jean-Gilles, R., Gadre, A., Cady, N. C., Yener, B., Castracane, J., & Larsen, M. (2012). The regulation of focal adhesion complex formation and salivary gland epithelial cell organization by nanofibrous PLGA scaffolds. *Biomaterials*, *33*(11), 3175–3186. https://doi.org/10.1016/j.biomaterials.2012.01.010

Sfakis, L., Kamaldinov, T., Khmaladze, A., Hosseini, Z. F., Nelson, D. A., Larsen, M., & Castracane, J. (2018). Mesenchymal Cells Affect Salivary Epithelial Cell Morphology on PGS/PLGA Core/Shell Nanofibers. *International Journal of Molecular Sciences*, *19*(4), 1031. https://doi.org/10.3390/ijms19041031

Shafiee, A., & Atala, A. (2017). Tissue Engineering: Toward a New Era of Medicine. *Annual Review of Medicine*, *68*, 29–40. https://doi.org/10.1146/annurev-med-102715-092331

Shao, F., Yu, L., Zhang, Y., An, C., Zhang, H., Zhang, Y., Xiong, Y., & Wang, H. (2020). Microfluidic Encapsulation of Single Cells by Alginate Microgels Using a Trigger-Gellified Strategy. *Frontiers in Bioengineering and Biotechnology*, *8*, 583065. https://doi.org/10.3389/fbioe.2020.583065

Song, Y., Zhang, C., Wang, P., Wang, L., Bao, C., Weir, M. D., Reynolds, M. A., Ren, K., Zhao, L., & Xu, H. H. K. (2017). Engineering bone regeneration with novel cell-laden hydrogel microfiber-injectable calcium phosphate scaffold. *Materials Science & Engineering. C, Materials for Biological Applications*, *75*, 895–905. https://doi.org/10.1016/j.msec.2017.02.158

Soscia, D. A., Sequeira, S. J., Schramm, R. A., Jayarathanam, K., Cantara, S. I., Larsen, M., & Castracane, J. (2013). Salivary gland cell differentiation and organization on micropatterned PLGA nanofiber craters. *Biomaterials*, *34*(28), 6773–6784. https://doi.org/10.1016/j.biomaterials.2013.05.061

Stokke, B. T. (2019). Polysaccharide Hydrogels. *Gels*, *5*(3), 38. https://doi.org/10.3390/gels5030038

Stokke, B. T., Draget, K. I., Smidsrød, O., Yuguchi, Y., Urakawa, H., & Kajiwara, K. (2000). Small-Angle X-ray Scattering and Rheological Characterization of Alginate Gels. 1. Ca−Alginate Gels. *Macromolecules*, *33*(5), 1853–1863. https://doi.org/10.1021/ma991559q

Teng, K., An, Q., Chen, Y., Zhang, Y., & Zhao, Y. (2021). Recent Development of Alginate-Based Materials and Their Versatile Functions in Biomedicine, Flexible Electronics, and Environmental Uses. *ACS Biomaterials Science & Engineering*, *7*(4), 1302–1337. https://doi.org/10.1021/acsbiomaterials.1c00116

Tibbitt, M. W., & Anseth, K. S. (2009). Hydrogels as extracellular matrix mimics for 3D cell culture. *Biotechnology and Bioengineering*, *103*(4), 655–663. https://doi.org/10.1002/bit.22361

Tortorella, I., Argentati, C., Emiliani, C., Martino, S., & Morena, F. (2022). The role of physical cues in the development of stem cell-derived organoids. *European Biophysics Journal: EBJ*, *51*(2), 105–117. https://doi.org/10.1007/s00249-021-01551-3

Watt, F. M., & Hogan, B. L. (2000). Out of Eden: Stem cells and their niches. *Science (New York, N.Y.)*, *287*(5457), 1427–1430. https://doi.org/10.1126/science.287.5457.1427

Wee, null, & Gombotz, null. (1998). Protein release from alginate matrices. *Advanced Drug Delivery Reviews*, *31*(3), 267–285. https://doi.org/10.1016/s0169-409x(97)00124-5

Xie, Y., Kollampally, S. C. R., Jorgensen, M., & Zhang, X. (2022). Alginate microfibers as therapeutic delivery scaffolds and tissue mimics. *Experimental Biology and Medicine (Maywood, N.J.)*, 15353702221112904. https://doi.org/10.1177/15353702221112905

Xue, J., Wu, T., Dai, Y., & Xia, Y. (2019). Electrospinning and Electrospun Nanofibers: Methods, Materials, and Applications. *Chemical Reviews*, *119*(8), 5298–5415. https://doi.org/10.1021/acs.chemrev.8b00593

Yamamoto, K., Yuguchi, Y., Stokke, B. T., Sikorski, P., & Bassett, D. C. (2019). Local Structure of Ca2+ Alginate Hydrogels Gelled via Competitive Ligand Exchange and Measured by Small Angle X-Ray Scattering. *Gels*, *5*(1), 3. https://doi.org/10.3390/gels5010003

Zdiri, K., Cayla, A., Elamri, A., Erard, A., & Salaun, F. (2022). Alginate-Based Bio-Composites and Their Potential Applications. *Journal of Functional Biomaterials*, *13*(3), 117. https://doi.org/10.3390/jfb13030117

Zhang, X., Xie, Y., Koh, C. G., & James Lee, L. (2009). A novel 3-D model for cell culture and tissue engineering. *Biomedical Microdevices*, *11*(4), 795–799. https://doi.org/10.1007/s10544-009-9294-8